ELSEVIER

Arthropod Structure & Development 33 (2004) 301–329

ARTHROPOD STRUCTURE & DEVELOPMENT

www.elsevier.com/locate/asd

Sensorimotor control of navigation in arthropod and artificial systems

Barbara Webb[a,*], Reid R. Harrison[b], Mark A. Willis[c]

[a]*School of Informatics Office, University of Edinburgh, 2 Buccleuch Place, Edinburgh EH8 9LW, Scotland, UK*
[b]*Department of Electrical and Computer Engineering, University of Utah, Salt Lake City, UT 84112, USA*
[c]*Department of Biology, Case Western Reserve University, Cleveland, OH 44106, USA*

Received 26 March 2004; accepted 14 May 2004

Abstract

Arthropods exhibit highly efficient solutions to sensorimotor navigation problems. They thus provide a source of inspiration and ideas to robotics researchers. At the same time, attempting to re-engineer these mechanisms in robot hardware and software provides useful insights into how the natural systems might work.

This paper reviews three examples of arthropod sensorimotor control systems that have been implemented and tested on robots. First we discuss visual control mechanisms of flies, such as the optomotor reflex and collision avoidance, that have been replicated in analog VLSI (very large scale integration) hardware and used to produce corrective behavior in robot vehicles. Then, we present a robot model of auditory localization in the cricket; and discuss integration of this behavior with the optomotor behavior previously described. Finally we present a model of olfactory search in the moth, which makes use of several sensory cues, and has also been tested using robot hardware. We discuss some of the similarities and differences of the solutions obtained.

Keywords: Biorobotics; Biomimetic; Cricket; Fly; Moth; Behavior

1. Introduction

Arthropods have been important in the study of sensorimotor control because of their relatively stereotyped, rapid responses and the possibility of closely connecting neural circuits to behavior. They have highly evolved sensory systems suited to specific task constraints. For example, the olfactory system of male moths is exquisitely tuned to the species-specific sex attractant synthesized by the females, and adapted to respond to the intermittent structure of odor plumes in natural environments. In addition it is evident that the physical anatomy of arthropod sensory systems plays an important role in the control process, as frequently they act as matched filters to extract critical variables. Examples include the receptive field arrays of visual neurons that make them responsive to rotational or looming signals, and the anatomy of the cricket auditory system, which produces good directionality, and is tuned to cricket song frequencies. Moreover, for several arthropod systems such as those discussed in this paper, we have excellent information about the direct connections between characteristics of identified neurons and the corresponding behavior of the animal. Much is known about the connection between visual neurons and flight torque, auditory interneurons and the walking response of the cricket, and descending visual interneuron activity modulated by pheromone and the associated odor-modulated flight steering.

Consequently, these systems have also been important in the fields of bio-mimetic engineering and robotics, providing not only inspiration but also specific design blueprints. When building robotic systems, we are directly faced with problems such as the inability to precisely control motion, particularly if dealing with uneven terrains or turbulent air; and with the need to deal with realistic, noisy, sensory input rather than the idealized signals that can be used in simulation. These are problems that insects have solved, and with the advantages of efficiency and low power. This suggests that such mechanisms are useful designs to adopt if attempting to build artificial systems with comparable capabilities.

However, though much is known about these biological systems, it is certainly not the case that they are fully explained or understood. The robot implementation will

* Corresponding author. Fax: +44-131-650-6626.
E-mail address: bwebb@inf.ed.ac.uk (B. Webb).

1467-8039/$ - see front matter © 2004 Elsevier Ltd. All rights reserved.
doi:10.1016/j.asd.2004.05.009

require a range of assumptions and additional hypotheses, as each part of the proposed mechanism must be made explicit if the system as a whole is to work. As a result, the robot embodies our current understanding of the biology, and thus enables us to test whether this is indeed adequate to explain the behavior. The robot becomes a test-bed for our hypothetical models of these systems, confronting them with realistic situations. Thus the robot results can usefully contribute to biological knowledge.

There is a surprisingly large body of work in the area of 'biorobotics' and overviews can be found in Webb (2000) and (2002). The interaction between biology and robotics seems to have been most productive in the area of basic sensory reflexes. Our first system to be discussed in detail, the optomotor and visual looming reflexes of flying insects, has been studied for many years and was one of the earliest examples of the application of cybernetic ideas to biology. Flies and other insects can use visual flow fields to stabilize their trajectories, and there appears to be a dedicated neural system for extracting relevant directions of flow and producing the appropriate output torque. The mechanisms can be efficiently replicated in analog electronics and used to stabilize robot trajectories under realistic conditions, even with extreme motor asymmetries.

Though the sound orienting behavior of the cricket is also very well studied, the functional model of the underlying neural processes is not so well developed as for the fly visual system. Female crickets can locate mates by walking or flying towards male calling songs. The carrier frequency and temporal pattern of the song will influence the orientation tendency, suggesting they are also recognizing conspecifics and discriminating their songs from other auditory signals. Constrained by what is known of the underlying anatomy and physiology, it is possible to design a simulated neural circuit that replicates the behavior when experimentally evaluated on a robot with a similar sensory system. The circuit is surprisingly simple and combines the two functions—localization and recognition—in a strongly integrated fashion.

Arthropods have many different modes of sensing, and some tasks demand the interaction of several modalities. One example is that auditory localization can be improved by incorporating visual stabilization mechanisms. We will describe the combination of these two sensory systems on a single robot base. This leads to interesting insights into how the nervous system can arbitrate between conflicting sensory signals. Olfactory tracking requires the interaction of chemical sensors, wind sensors and visual information; and unlike the auditory tracking or optomotor response, cannot be purely reactive but also requires some memory. For a male moth attempting to follow a pheromone plume dispersed by the wind from the female, the signal does not form a convenient gradient but is turbulent and patchy. The basic mechanism seems to involve the animal turning up wind when it encounters the chemical cue, and executing a 'program' of turns that is modulated by further encounters. The nature of this program can be explored using a robot with equivalent sensors and testing its behavior in the same experimental situation as the moth with different control algorithms.

In what follows, we will describe each of these biological systems in more detail, explain how the hypotheses about their function were implemented on robots, and report the resulting robot behavior when tested in natural or experimental situations that resemble the animal's task. We will then discuss some of the similarities and differences between the systems, and how the work has influenced our understanding of sensorimotor control mechanisms.

2. Visually-guided navigation

2.1. Background

2.1.1. Behavior

Flies rely heavily on visual motion information to survive. In the fly, motion information is known to underlie many important behaviors including stabilization during flight, orienting towards small, rapidly moving objects (Egelhaaf and Borst, 1993), and estimating time-to-contact for safe landings (Borst and Bahde, 1988). Some motion-related tasks like extending the legs for landing can be executed less than 70 ms after stimulus presentation. Wagner reports a 30 ms reaction time for male flies chasing prospective mates (Wagner, 1986). The computational machinery performing this sensory processing is fast, small, low power, and robust.

Flies use visual motion information to estimate self-rotation and generate a compensatory torque response to maintain stability during flight. This well-studied behavior is known as the optomotor response. It is interesting from an engineering standpoint because it extracts relevant information from a dynamic, unstructured environment on the basis of passive sensors and uses this information to generate appropriate motor commands during flight. This system is implemented in biological hardware that is many orders of magnitude smaller and more power efficient than CCD imagers coupled to a conventional digital microprocessor.

Much of the computation underlying the optomotor control system is performed by the 'HS cells' (Geiger and Nässel, 1981; Geiger and Nässel, 1982; Egelhaaf et al., 1988; Hausen and Wehrhahn, 1990; Egelhaaf and Borst, 1993) described in more detail below. This well-studied system estimates rotation from optic flow and uses this information to produce a stabilizing torque with the wings (Götz, 1975; Warzecha and Egelhaaf, 1996).

Flies also use visual motion information to coordinate landings. Behavioral and modeling studies indicate that such 'time-to-landing' estimation could be produced by a temporal integration of the output of neurons sensitive to expanding optic flow patterns (Borst and Bahde, 1988; Borst, 1990). A similar visual capability allows flies to avoid rapidly approaching predators. This escape response

is sensitive to motion as well as to decreases in light intensity (Holmqvist and Srinivasan, 1991).

2.1.2. Anatomy and physiology

In the housefly's brain, over half of the 350,000 neurons are believed to have some role in visual processing. Insects process visual motion information in a local, hierarchical manner. Photoreceptors in the retina adapt to the ambient light level, and signal temporal deviations from this level. These signals are passed on to the next layer of cells, the lamina (Fig. 1). Lamina cells generally show transient or highpass responses, emphasizing temporal change (Weckström et al., 1992). The next stage of processing is the medulla, a layer of cells that are extremely difficult to study directly due to their small size. Indirect evidence suggests that local measures of motion (i.e. between adjacent photoreceptors) are computed here: hence the cells are described as 'elementary motion detectors' (EMDs). These local, direction-selective motion estimates are integrated by large tangential cells in the lobula plate (Hausen and Egelhaaf, 1989). The housefly has 50–60 tangential cells in each hemisphere of its brain. These are the best-studied cells in the fly visual system, and much is known about their properties. Many of these neurons have been linked to specific visually-guided behaviors that help the animal navigate through a complex environment in a robust manner (Egelhaaf and Borst, 1993).

Each eye of the blowfly *Calliphora erythrocephala* consists of approximately 6000 individual lenses. Despite the multi-lens construction of the compound eye, the pattern projected onto the underlying retina is a single image of the visual scene. Beneath each lens is a cluster of eight light-sensitive cells. Each lens and its associated photoreceptors form a unit called an ommatidium. Six of the eight photoreceptors are used to implement neural superposition, a technique to increase the effective lens diameter by pooling the responses of neighboring ommatidia. The other two photoreceptors do not seem to be involved in the detection of motion. Mutants with these photoreceptors impaired cannot discriminate colors, but show no motion-related

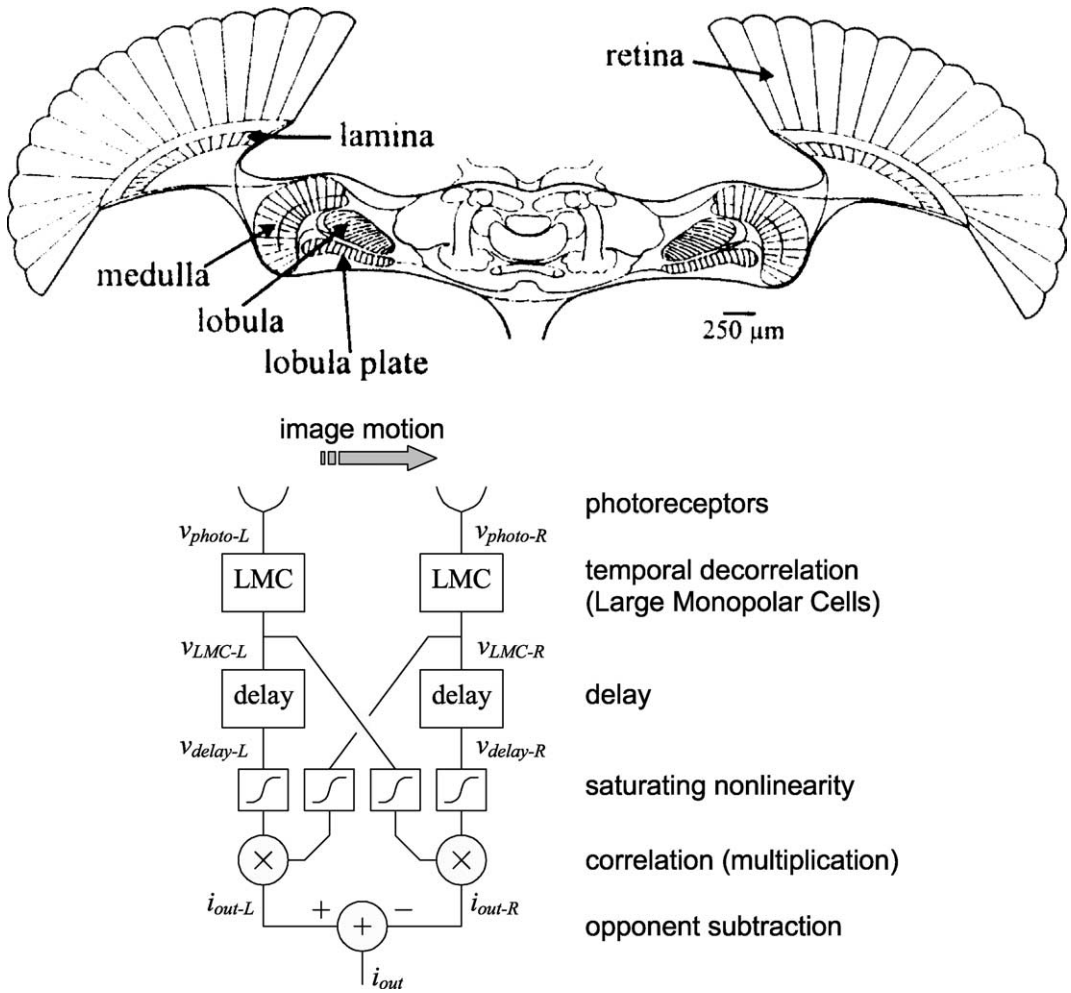

Fig. 1. (Top) Anatomy of the fly visual system. Lenses in each compound eye focus light onto the retina. Photoreceptor signals are transmitted to the lamina, which emphasizes temporal change. Motion detection is performed in the medulla, lobula, and lobula plate. Adapted from Borst and Haag, 1996. (Bottom) Elaborated delay-and-correlate elementary motion detector (EMD) model. The signal from one photoreceptor is correlated with the delayed signal from an adjacent photoreceptor. Direction selectivity is increased by subtracting the responses of two half-detectors in opponency.

deficits (Heisenberg and Buchner, 1977). From an information-processing perspective, each ommatidium records one 'pixel' of the external world's image. Interommatidial angular spacing is 1.1–1.3° (Land, 1997). This angular resolution is approximately 150 times worse than the 0.008° resolution in foveated region of the human retina (Wandell, 1995). While inferior to human eyes spatially, fly vision far exceeds ours temporally. Human vision is sensitive to temporal modulations up to 20 or 30 Hz, while fly photoreceptors respond to temporal frequencies as high as 300 Hz (Autrum, 1958).

The laminar region, also called the first optic ganglion, contains cells that exhibit transient responses to step intensity changes. The large monopolar cells (LMCs) in this ganglion ignore the dc light level but amplify temporal changes (Weckström et al., 1992). This highpass response has been shown to optimize information transfer through this region (Laughlin, 1994). Laminar cells do not exhibit motion-specific responses. There is a strong retinotopic organization from the retina through the lamina to the next layer, the medulla (Fig. 1). Every ommatidium has an associated neural 'cartridge' beneath it in these underlying ganglia, suggesting many identical processing units operating in parallel (Strausfeld, 1976). Cells in this second optic ganglion are extremely small and difficult to record from, and little is known about their structure or function. DeVoe recorded from medullar cells in *Calliphora* and reported a wide variety of response characteristics: transient temporal responses, sustained responses, directional motion responses, and nondirectional motion responses (DeVoe and Ockleford, 1976; DeVoe, 1980).

The third optic ganglion is also known as the lobula–lobula plate complex (Fig. 1). At this point in the optic lobe, the retinotopic organization ends with massive spatial convergence. Information from several thousand photoreceptors converges onto 50–60 tangential cells. These cells have broad dendritic trees that receive synaptic input from large regions of the medulla, resulting in large visual receptive fields (Hausen, 1982a,b; 1984; Hengstenberg, 1982; Krapp and Hengstenberg, 1996).

A subset of these neurons were found to respond primarily to horizontal motion, and these cells were given names beginning with 'H'. H1 is a spiking neuron that responds to back-to-front optic flow. HSS, HSE, and HSN are graded potential (nonspiking) neurons covering the southern, equatorial, and northern regions of the visual field, respectively. Collectively called the HS cells, these neurons are depolarized by full-field visual motion from the front to the back of the eye, and hyperpolarized by back-to-front motion. They have been shown to encode horizontal motion as effectively as the spiking H1 cell (Haag and Borst, 1998). Each HS cell integrates signals from an ipsilateral retinotopic array of elementary motion detectors (EMDs), units in the medulla that estimate local motion in small areas of the visual field. The HS cells synapse onto descending, spiking neurons, which relay information to the motor centers of the thoracic ganglion. Another class of neurons, the VS cells, responds to vertical motion. Recently, it has been shown that these HS and VS cells are not simply responsive to motion along one axis, but rather act as matched filters for complex patterns of optic flow that would be produced by body rotations (Krapp and Hengstenberg, 1996).

Four 'figure detectors', or FD neurons, have also been identified in the lobular plate. These cells respond more vigorously to small moving objects than to full-field motion (Egelhaaf, 1985). These are thought to underlie the ability to discriminate objects from background using relative motion (parallax) cues (Kimmerle et al., 1996, 1997) which has been demonstrated in behavioral experiments both with freely flying and tethered flies.

2.2. Designs

2.2.1. Elementary motion detector design

Beginning with the pioneering work of Franceschini and colleagues, models of EMD function were implemented using discrete electronic circuits on mobile robots (Pichon et al., 1989; Franceschini et al., 1992). Over the past decade, analog integrated circuit designers have developed integrated silicon versions of these EMD circuits and used these chips for control tasks including optomotor stabilization and collision detection (Moini et al., 1997; Harrison and Koch, 1999; 2000a,b; Liu and Usseglio-Viretta, 2001; Harrison, 2003). This work originated from the pioneering neuromorphic engineering work by Carver Mead in the 1980s (Mead, 1989).

We use an enhanced version of the familiar delay-and-correlate or 'Reichardt' EMD first proposed by Hassenstein and Reichardt in the 1950s to explain the optomotor response of beetles (Hassenstein and Reichardt, 1956). Fig. 1 shows a diagram of the EMD used in our very large scale integration (VLSI) sensors. The first stage of the EMD is photoreception, where light intensity is transduced to a voltage signal v_{photo}. Since light intensity is a strictly positive value, the mean intensity of the scene must be subtracted. Since we are interested in motion, it is also advantageous to amplify transient signals.

Suppressing dc illumination and enhancing ac components of photoreceptor signals is a common theme in many biological visual systems. In flies, large monopolar cells (LMCs) directly postsynaptic to photoreceptors exhibit transient biphasic impulse responses approximately 40–200 ms in duration (Laughlin, 1994; van Hateren, 1992). In the frequency domain, this can be seen as a bandpass filtering operation that attenuates dc signals while amplifying signals in the 2–40 Hz range (van Hateren, 1992, 1997). In the lateral geniculate nucleus of cats, 'lagged' and 'non-lagged' cells exhibit transient biphasic impulse responses 200–300 ms in duration and act as bandpass filters amplifying signals in the 1–10 Hz range (Saul and Humphrey, 1990). This filtering has recently been explained

in terms of temporal de-correlation, and can be seen as a way of removing redundant information from the photoreceptor signal before further processing (van Hateren, 1992; Dong and Atick, 1995).

After this 'transient enhancement', or temporal de-correlation, the signals are delayed using the phase lag of a lowpass filter. While not a true time delay, the lowpass filter matches data from animal experiments and makes the Reichardt EMD equivalent to the oriented spatiotemporal energy filter proposed by Adelson and Bergen (Adelson and Bergen, 1985). Before correlating the adjacent delayed and non-delayed signals, we apply a saturating static nonlinearity to each channel. Without such a nonlinearity, the delay-and-correlate EMD exhibits a quadratic dependence on image contrast. In fly tangential neurons, motion responses show a quadratic dependence only at very low contrasts, then quickly become largely independent of image contrast for contrasts above 30%. Egelhaaf and Borst proposed the presence of this nonlinearity in the biological EMD to explain this contrast independence (Egelhaaf and Borst, 1989). Functionally, it is necessary to prevent high-contrast edges from dominating the summed output of the EMD array.

After correlation, opponent subtraction produces a strong directionally selective signal that is taken as the output of the EMD. Unlike algorithms that find and track features in an image, the delay-and-correlate EMD does not measure true image velocity independent of the spatial structure of the image. However, recent work has shown that for natural scenes, these Reichardt EMDs give reliable estimates of image velocity (Dror et al., 2001). This reliability is improved by the addition of LMC bandpass filters and saturating nonlinearities. Experiments using earlier versions of silicon EMDs have demonstrated the ability of delay-and-correlate motion detectors to work at very low signal-to-noise ratios (Harrison and Koch, 2000a).

2.2.2. Optomotor control system

We constructed an optomotor feedback loop using a VLSI wide-field motion sensor with a 30° field of view (Harrison and Koch, 1999). The sensor was mounted facing forward on a robot, oriented so it was sensitive to horizontal motion. The robot had two large wheels driven independently by two DC motors, and a free-turning wheel in the back to maintain balance (not shown). Each drive motor was controlled with a pulse-width modulation circuit that varied the duty cycle of a constant-amplitude square wave voltage. By changing the duty cycle of the waveform, each motor could be driven at any speed up to a maximum. If the motors were driven at different speeds, the robot would drive in a curved trajectory.

We oriented the sensor facing straight ahead since translatory motion by the robot produces little optic flow in the direction of travel, while rotatory (yaw) motion produces uniform optic flow around the visual field parallel to the ground. Thus the optic flow in the forward region of the visual field will be dominated by the rotatory component. The hoverfly *Syritta pipiens* uses this strategy to stabilize its flight. When moving forward, the animal uses optic flow from the forward region of the visual field to estimate self rotation. This agile creature is also capable of flying sideways, and when doing so it uses optic flow from the lateral visual fields to estimate self rotation (Collett, 1980a). Presumably, it is attempting to measure optic flow in the regions least contaminated with optic flow produced by its own translation.

The output of our motion sensor was a continuous, time-varying voltage. This signal was filtered by a first-order lowpass filter with a time constant of 750 ms. This is a simple model of the relationship between the output of a wide-field motion-sensitive neuron in the fly and the torque response produced by the wings (Egelhaaf, 1987; Warzecha and Egelhaaf, 1996). The filtered output of the motion sensor was added to the robot's left motor command and subtracted from its right motor command (see Fig. 2A). This has the effect of adding a rotatory component to the robot's trajectory that is directly proportional to the sensed visual motion velocity.

2.2.3. Collision detection system

While several models have been proposed to explain collision detection, the model proposed in (Borst and Bahde, 1988) is particularly amenable to hardware implementation. The model, shown in Fig. 2B, employs a radially oriented array of motion detectors centered in the direction of flight. As the animal approaches a static object, an expansive optic flow field is produced on the retina. A wide-angle field of view is useful since optic flow in the direction of flight will be zero. The response of this radial array of motion detectors is summed and then passed through a leaky integrator (a lowpass filter). If this response exceeds a fixed threshold, an imminent collision is detected and the animal can take evasive action or prepare for a landing. This expansive optic flow model has recently been used to explain landing and collision avoidance responses in the fruit fly (Tammero and Dickinson, 2002). A similar algorithm has been implemented in a computer simulation for autonomous robot navigation (Duchon et al., 1998). We developed a single-chip analog VLSI sensor to implement this model (Harrison, 2003). Other models proposed for collision detection (Wagner, 1982) typically require the size of the approaching object to be computed. These algorithms require an additional visual subsystem for identifying the object and segmenting it from the background. This is not a trivial task in complex visual scenes.

To build a collision detector, we fabricated a 16×16 EMD array in a 0.5-μm 2-poly, 3-metal standard CMOS process. The $2.24\,\text{mm} \times 2.24\,\text{mm}$ die contained a 17×17 array of 'pixels', each measuring $100\,\mu\text{m} \times 100\,\mu\text{m}$ (see Fig. 4). Each pixel contained a photoreceptor, LMC circuit, lowpass 'delay' filter, and four correlators. These correlators were used to implement two independent EMDs: a vertical motion detector connected to the pixel below and a horizontal motion

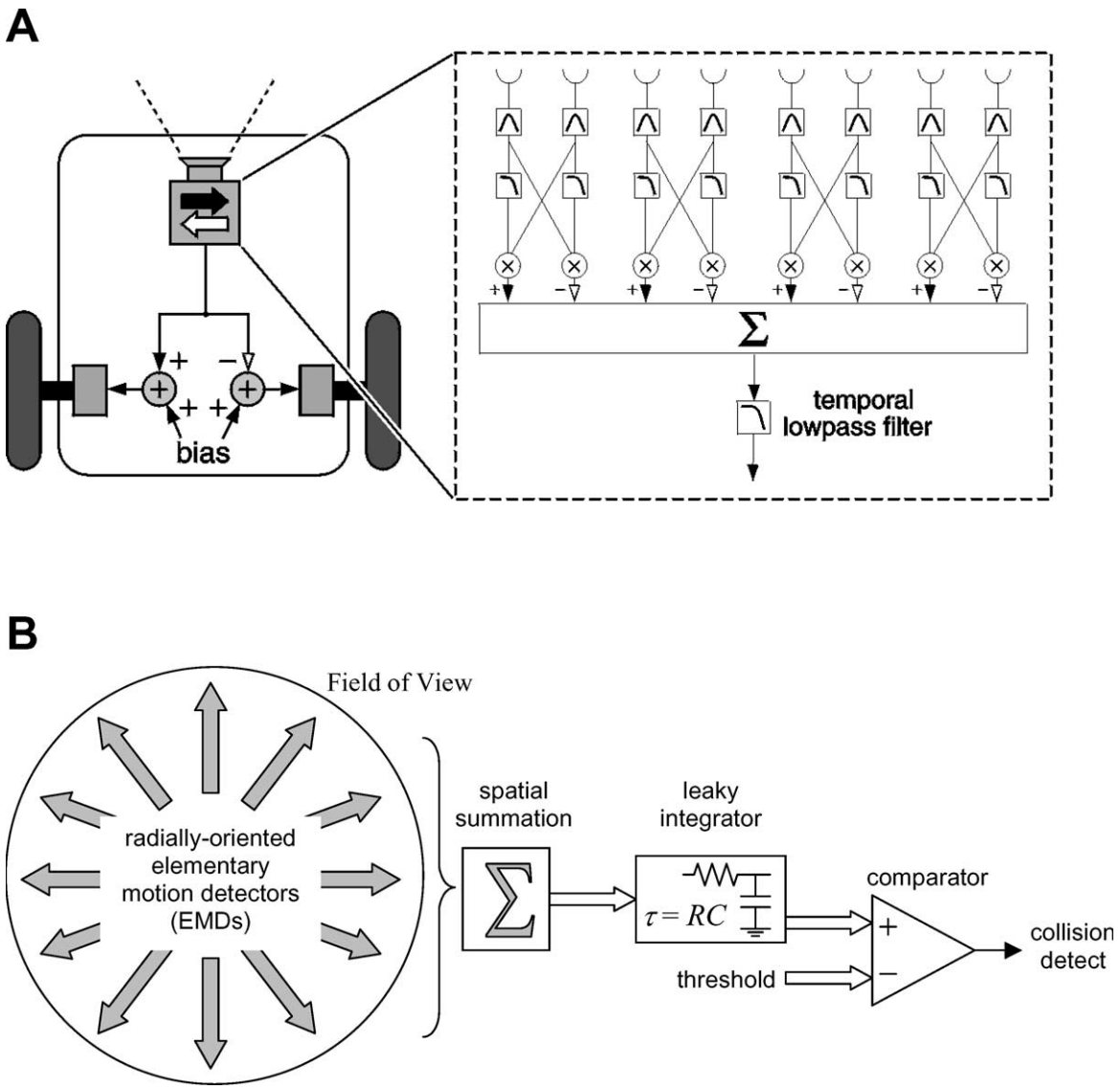

Fig. 2. A. Schematic of optomotor system for controlling robot. A motion sensor chip is mounted facing forward on a robotic platform. The forward-looking motion sensor is largely blind to optic flow produced by forward translation, so only rotation is measured. The sensory signal is added to one motor and subtracted from another to yield a compensatory rotation. A constant motor bias produces forward translatory motion. B. Diagram of collision detection algorithm. The model employs a radially oriented array of motion detectors centered in the direction of flight. As the agent approaches a static object, an expansive optic flow field is produced on the retina. The response of the motion detector array is summed and passed through a leaky integrator. If this response exceeds a fixed threshold, an imminent collision is detected and the agent can take evasive action or prepare for a landing.

detector connected to the pixel to the right. The output signals from a subset of the EMDs representing radial outward motion were connected to two global wires, giving a differential current signal that was taken off chip on two pins.

The entire chip consumed 140 μW of power. Most of this was consumed by peripheral biasing circuits; the 17×17 pixel array used only 5.2 μW (18 nW per pixel). To test the complete collision detection chip, we implemented the leaky integrator ($\tau_{leak} = 50$ ms) and comparator from Fig. 2B using off-chip components. In future implementations, these circuits could be built on chip using little power.

2.3. Results

2.3.1. Optomotor robot experiments

To test the efficacy of the optomotor system, a large asymmetry was introduced into the robot's mechanics by connecting the left and right motors to their respective wheels with different gear ratios. The left motor was connected to the left wheel with a 1:5 gear ratio, while the right motor was connected to the right wheel with a 1:1 gear ratio. This caused the robot to drive in tight circles if both motors were driven at the same speed. This asymmetry was made extreme for the sake of experiment, but perfect symmetry is impossible to achieve in any physical robot.

While two actuators may match perfectly in simulation, they will never match when built and tested in the real world. This difficulty is especially pronounced in outdoor terrain, where wheels or feet may slip in sand or mud. Legged robots are especially prone to walking in curved lines due to foot slip or terrain differences, even if they have been designed and constructed with high precision. Similar problems are faced by walking insects, and flying insects generally have to compensate for many asymmetries; wind deflection is a particularly critical problem.

Experiments were performed indoors in our laboratory, but the visual nature of the room was not altered in any way to accommodate the motion sensor. The room was a typical cluttered laboratory environment with many shady areas under tables. The robot's position was recorded 10–20 times per second with a magnetic field tracking system that returned location and orientation in three dimensions (Polhemus, Colchester, VT). The scale of experiments was limited by the range of this system, approximately a 70 cm × 140 cm area for highest accuracy.

The optic flow feedback proved capable of nearly eliminating the effect of physical asymmetry. Fig. 3A shows one trial without visual feedback. The line shows the robot's path, and the circle indicates the ending position. The robot is turning in tight circles. Fig. 3B shows ten trials where visual feedback has been enabled. In general, the robot travels in straight lines. We purposely started the robot at different orientations to demonstrate that the sensor works well for general visual scenes around a room. When moving in straight lines, the robot traveled at a speed of approximately 20 cm/s. Objects and walls were typically 0.2–1.5 m away from the robot, depending on the direction.

The angular velocity of the robot (yaw rate) was computed along each path by differentiating the robot's heading as recorded by the tracking system. The mean angular velocity in the open-loop case is −116 deg/s, while for the closed-loop case this decreased to −3.7 deg/s, an improvement by a factor of 31.

Occasionally, the feedback did fail to keep the course straight. A 45° turn is visible in Fig. 3B, most likely caused by the sensor being oriented toward a relatively featureless part of the room, where no motion information is available. A larger field of view would reduce the likelihood of such occurrences. Also, the magnitude of the error depends on the degree of asymmetry in the gear ratios. In a more realistic situation with higher open-loop precision, it is likely that large closed-loop errors would be rare.

2.3.2. Collision detector experiments

We tested the collision detection chip described in Section 2.2.3 by mounting two on a small motorized vehicle similar to the one shown in Fig. 4B, facing forward with the lenses centered 11 cm above the floor. Unlike the vehicle used in optomotor experiments, this vehicle was mechanically balanced with no bias to turn clockwise or counterclockwise. Improved optics gave this chip a 140° field of view. The vehicle traveled in a straight path at 28 cm/s. Fig. 4C shows the output from the leaky integrator as the chip moves across the floor and collides with the center of a 38 cm × 38 cm metal box in our lab. The peak response of the chip occurs approximately 500 ms before contact, which corresponds to a distance of 14 cm. At this point, the edges of the box subtend an angle of 54°. After this point, the edges of the box move beyond the chip's field of view, and the response decays rapidly. The rebound in response observed in the last 100 ms may be due to the chip seeing the expanding shadow cast by its own lens on the side of the box just before contact. We use a simple comparator to detect imminent collision when the response exceeds a fixed threshold.

As shown in Fig. 4C, the time course of the output signal has a distinct shape, peaking before collision and then collapsing. This is similar to the activity patterns observed in LGMD neuron in locusts (Gabbiani et al., 1999) and η neurons in pigeons (Sun and Frost, 1998) during simulated collisions.

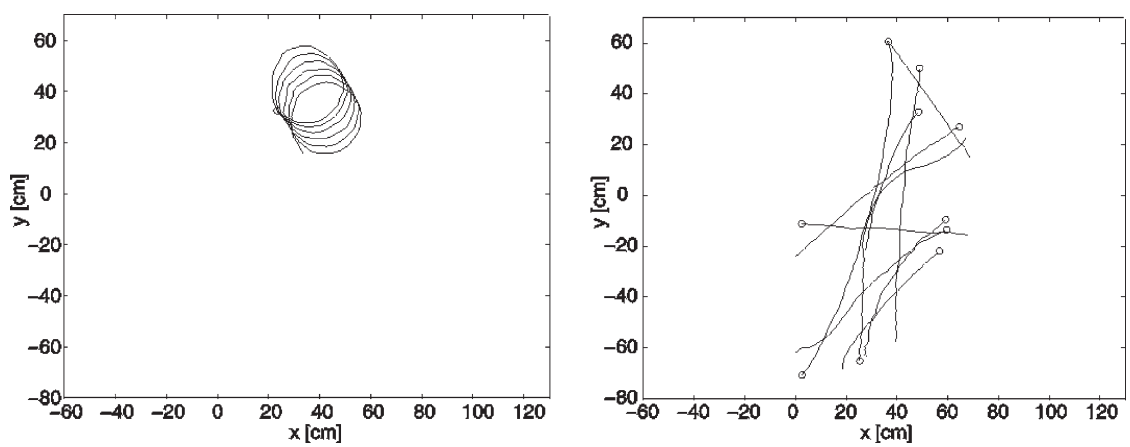

Fig. 3. Optomotor robot experiments. (Left) Robot path with no sensory feedback. With the motion sensor disabled, the robot turns in circles due to the asymmetry in its mechanics. (Right) Robot path with sensory feedback from optomotor sensor. Ten trials are shown.

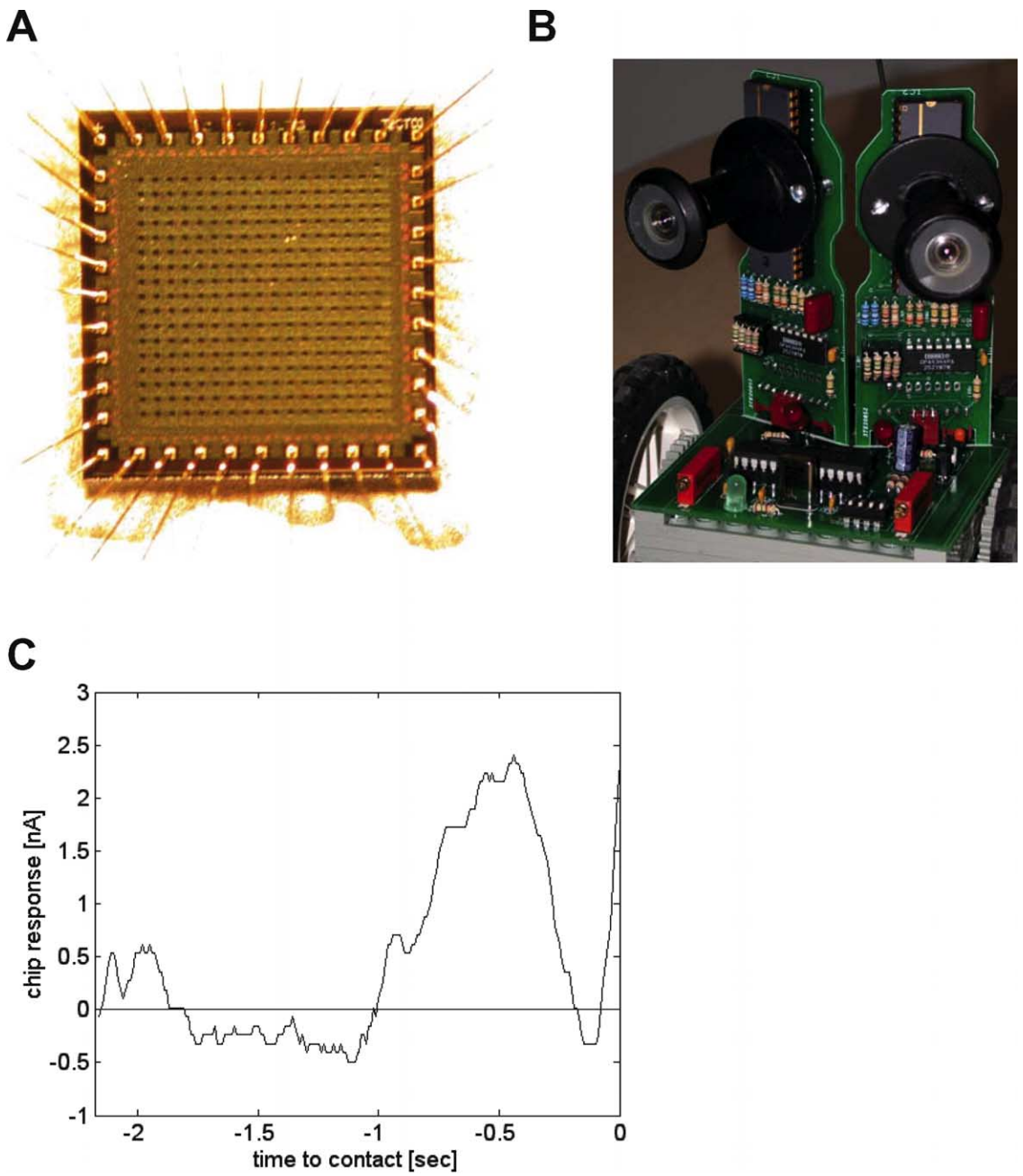

Fig. 4. A. Collision detector chip measuring 2.2 mm × 2.2 mm. The chip contains a 17 × 17 array of photoreceptors with motion detectors between neighboring cells. The chip consumes 140 μW of power. B. Small robotic vehicle with two collision detector chips mounted behind wide-angle lenses (black structures). For scale the round lens housings are 2.5 cm in diameter. C. Measured output of collision detection chip after off-chip leaky integration. The peak response of the chip occurs approximately 500 ms before contact, which corresponds to a distance of 14 cm from the obstacle.

3. Auditory-guided navigation

3.1. Background

3.1.1. Behavior

Cricket males produce calling songs of a characteristic frequency and temporal pattern and female crickets can find males using this cue alone. The song is produced by the male closing its wings, which rubs a comb on one against a plectrum on the other, with the sound being amplified by a resonant area on the wing (Bennett-Clark, 1989). The carrier frequency of the song corresponds to the rate at which the teeth of the comb pass over the plectrum, and is around 4–5 kHz for most cricket species. The temporal pattern consists of regularly repeated bursts of sound ('syllables') corresponding to each closing of the wings, followed by a silent interval as the wings open again. In *Gryllus bimaculatus*, for example, this results in a syllable duration of around 20 ms, followed by a gap of similar duration. There is an additional level of temporal pattern with the

syllables occurring in groups (chirps) of three or four, followed by a silent period of around 200–500 ms. These temporal patterns vary for different cricket species, and thus provide a basis by which females might recognize conspecifics.

Substantial experimental evaluation of the behavior of female crickets to different sound sources has been carried out, usually employing one of three methods: free walking in an arena (e.g. Stout and McGhee, 1988); a fixed body but legs or abdomen able to move and thus indicate attempted steering movements (e.g. Stabel et al., 1989; Pollack, 1986); and walking freely on a sphere in a 'Kramer' treadmill that compensates for the movement (e.g. Schmitz et al., 1982; Weber and Thorson, 1988). The most consistent finding is that crickets steer most directly to songs of a specific carrier frequency and syllable repetition rate. Thorson et al. (1982) have argued that, given the right carrier frequency, the rate of repetition of the syllables within the chirp is the only temporal parameter essential for taxis in female *Gryllus campestris*. Stout and McGhee (1988) similarly found that for *Acheta domestica* the repetition rate of syllables strongly affected the direction of taxis when syllable length and number of syllables per chirp were held constant, with rates of 15–20 Hz more effective than faster or slower rates. They found that syllable length, syllables per chirp, and chirp rate had a lesser, though not negligible effect. Pollack and Hoy (1981) found that for *Teleogryllus*, a continuous sequence of syllables at around 15 Hz was more effective in producing taxis than the actual conspecific song pattern which includes more complex patterns. Wendler (1990) found that for *Gryllus bimaculatus* a tone sinusoidally modulated at 30 Hz, i.e. at the typical syllable rate, produced directed taxis when 17 or 50 Hz did not; however, he also found significant taxis towards 3 Hz modulation, i.e. at the typical chirp rate. Thus, for all these species, selectivity for the syllable repetition rate is a common feature that needs to be explained.

Till recently, the accepted model for this behavior (see e.g. Horseman and Huber, 1994; Pollack, 2001) was that the cricket's auditory system needed to a) filter for the correct carrier frequency and syllable rate, and if the song is recognized use b) a strategy of turning to the side where sound is louder. The frequency filtering is thought to result largely from frequency tuning in receptors. The recognition of syllable rate is thought to involve brain neurons with high-pass, low-pass and band-pass filter responses (Schildberger, 1984; Huber and Thorson, 1985). Deciding which side is louder is thought to involve a comparison of firing rates in auditory interneurons (Horseman and Huber, 1994). Our modeling experiments (discussed below) and recent experiments on the cricket (Nabatiyan et al., 2003) have suggested some alternative solutions.

3.1.2. Anatomy and physiology

The cricket's ears are a pair of tympani, on each front leg, which are connected to each other and to a pair of spiracles on either side of the prothorax by a set of tracheal tubes (Fig. 5A). Because the cricket is small relative to the wavelength and distance of the sound it is trying to localize, there is little difference in the external amplitude of sound at the left and right tympani. However, sound also reaches the internal surface of the tympani from the other auditory ports after delay and filtering in the tracheal tubes. The vibrations of the tympani are thus determined by the combination of filtered delayed and direct sounds (Michelsen et al., 1994). Depending on the frequency of the signal and the direction of the sound, the phase of the delayed sounds will be shifted (relative to the direct sound) differentially for the two tympani, so that the amplitude of the summed signals will differ, even though the amplitude of the direct signals is similar. For a fixed frequency, the resulting amplitude difference indicates the direction of the sound.

There are several points to note about this mechanism. One is that it is a very effective means for detecting sound direction when the physical and processing capacities of the animal can support neither sound-shadowing nor phase-locked neural comparison, the two main cues for sound localization in vertebrate systems. A second is that, because the delays are fixed, it functions effectively only around a particular frequency. This could potentially contribute to the carrier frequency selectivity found in female cricket behavior, as discussed below.

Around 50–60 sensory neurons innervate each tympanum, with perhaps half of these tuned to the calling song frequency (Esch et al., 1980). Their axons traverse the leg nerve to the prothoracic ganglion. One pair of identified ascending interneurons ('AN1') in the cricket's prothoracic ganglion appears to be critical for phonotaxis (Schildberger and Hörner, 1988). AN1 respond best to sound at the calling song carrier frequency, and clearly encode the pattern of the song in their spiking response. Hyperpolarizing one of the pair leads to a change in walking direction. A second pair of neurons that receive input from the auditory nerve are the omega neurons (ON1) (Wohlers and Huber, 1981). These are mutually inhibitory and also inhibit the opposite ascending interneurons (Horseman and Huber, 1994). The most obvious function of these connections is to increase the difference in activation between the two sides, to emphasize the directionality of the response. The ON1 neurons also exhibit a slow, calcium-mediated adaptation that may act as a gain control mechanism (Sobel and Tank, 1994). There are a number of other auditory interneurons in the prothoracic ganglion but their functional role in phonotaxis has not been so clearly characterized. Some are known to be involved in ultrasound escape behavior.

The ascending neurons project to the protocerebrum. The most comprehensive study of the role of cricket brain neurons in phonotaxis is provided by Schildberger (1984), who suggests a possible filtering circuit for syllable rate recognition by the female. He identifies two main classes of auditory responsive cells: BNC1 which appear to get direct input from AN1; and BNC2 which get input via BNC1. Neurons within these classes vary in their response to the

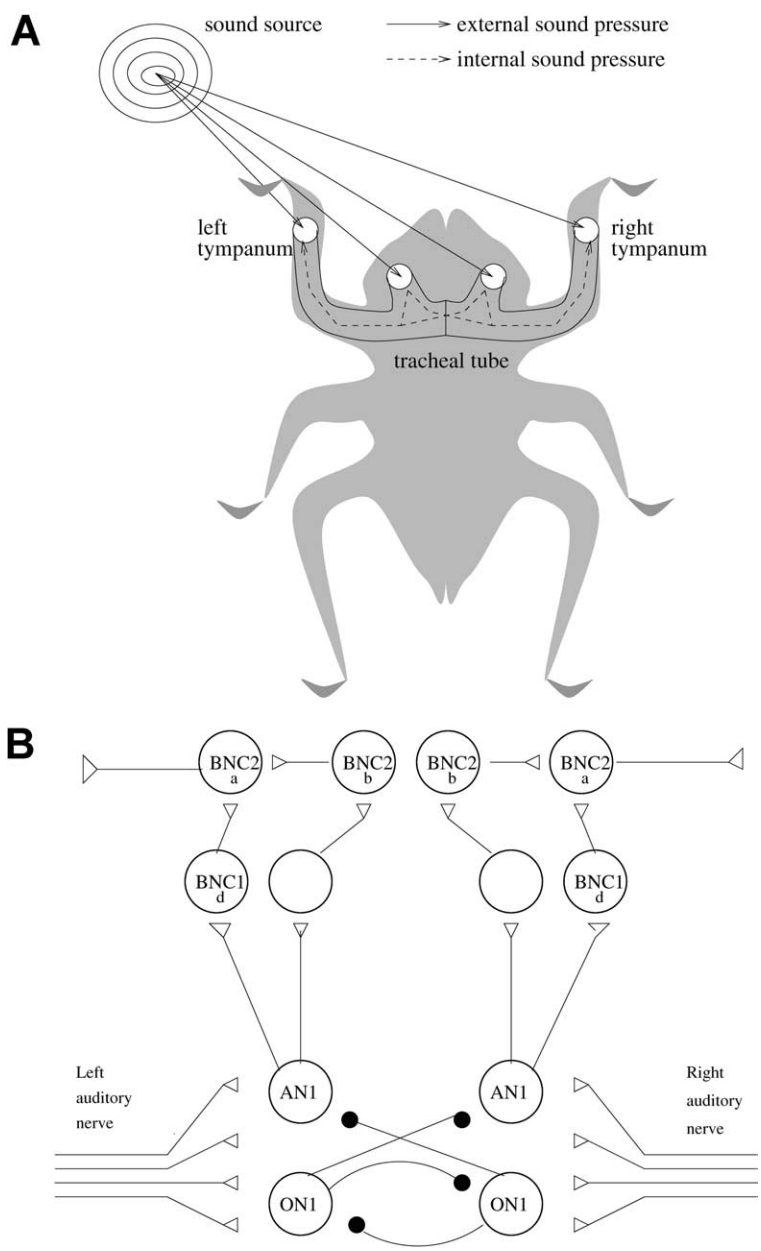

Fig. 5. A. A schematic diagram of the anatomy of the cricket auditory system. The tympani on the legs and the spiracles on the body are connected by a tracheal tube. Thus the vibration of each tympanum is a sum of direct and indirect sound waves. The phase differences resulting from the different distances traveled by the components of this sum cause the amplitude of tympanal vibration to be direction dependent. B. The main neural connections shown to be involved in the cricket phonotaxis response (see text for details). For this and subsequent figures, open triangles are excitatory synapses and closed circles are inhibitory.

pattern of sound. BNC1d appears to require a minimum syllable duration near to the typical calling song before it reaches threshold, which makes it a low-pass filter for the syllable rate, assuming a constant duty cycle. BNC2b appears to spike around once per syllable, which makes it high-pass i.e. as the syllable rate decreases the firing rate will also decrease. BNC2a shows band-pass filtering, responding at somewhat less than a spike per syllable for normal rates but producing fewer spikes for slow rates or fast rates. Schildberger (1984) argues that the response of BNC2a could be the result of a logical 'AND' operation on the output of BNC2b and BNC1d, to produce a neural recognition signal for the appropriate sound pattern. A schematic illustration of the critical neural connections is given in Fig. 5B.

Staudacher and Schildberger (1998); Staudacher (2001) have described properties of some descending neurons, many of which show a response to sound. The response to calling songs is typically 'gated' by whether or not the animal is walking. One of these neurons has a firing rate that correlates with the angular velocity of the animal, and another seems to be necessary and sufficient for the onset of

walking. However the evidence is not sufficient to determine with any clarity the output circuitry for phonotaxis.

3.2. Designs

3.2.1. Ears sensor

We have modeled the auditory morphology of the cricket using a programmable electronic circuit (Fig. 6). In a simplified approach, two microphone inputs are used. Each is delayed, inverted and then combined with the other to form a composite response. The distance between the two inputs was set at 18 mm, that is, approximately 1/4 of the wavelength of the cricket song carrier frequency of 4.7 kHz, and the delay between them set to 53 μs, the time for sound to propagate the distance between the microphones. Thus the direct and delayed inputs to the sum will be 180° out of phase if the sound is on the same side as the direct input, so the combined response will be amplified. If sound is on the opposite side, the direct and delayed inputs will be in phase and thus cancel out. The relative phase, and corresponding amplitude of the combined signal, will vary between these two extremes as the sound direction changes. The amplitude of the composite response is measured by an RMS circuit and converted from analogue to digital to be read by the robot's microprocessor.

The actual electronic circuit we are using has a more complex design, with the possibility of using four microphones to represent both tympani and spiracles, and

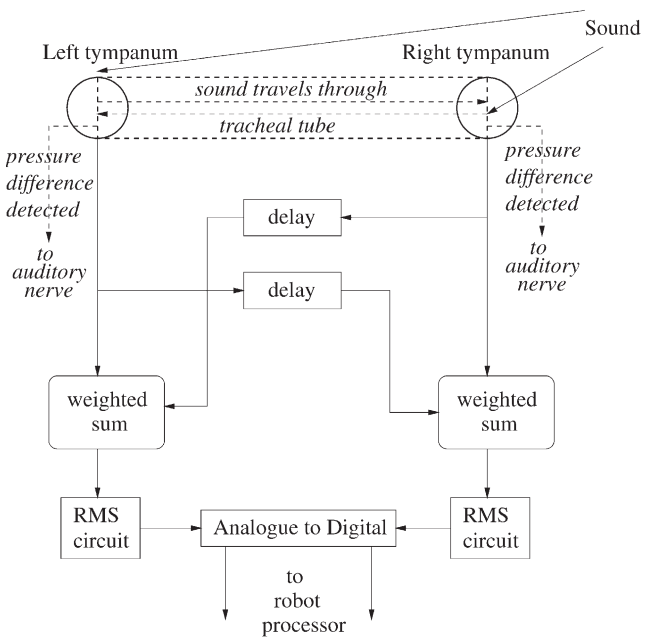

Fig. 6. The cricket auditory system shown in Fig. 9 can be simplified to a two input pressure difference receiver. This can be mimicked electronically using two microphones. The input of each is delayed and then combined with the other in a weighted sum. The amplitude of the resulting signal is obtained using an RMS circuit, and the analog signal then converted to digital to be used by the robot's microprocessor.

of programming the pre-amplification gains, delays, and weightings of the components of the sum at each tympanum to match those measured for the cricket (see Lund et al., 1997). In current experiments we are testing whether there is any behavioral advantage gained by incorporating these details, but in the experiments described here the circuit was used in the simpler two input mode as specified above.

3.2.2. Spiking neuron simulation of auditory processing

We have implemented a number of different simulations of the auditory processing of the cricket, starting with simple algorithms, but gradually incorporating more of the neurophysiological detail described above. Our most recent model (described in full detail in Reeve and Webb, 2003) uses integrate-and-fire neurons similar to those described by Koch (1999). Each neuron is represented as a resistor–capacitor (RC) circuit with a base potential towards which it decays exponentially in the absence of external input. If the membrane potential rises above a threshold, the neuron will 'fire', sending a spike to any output synapses, and then reset the membrane potential to a specified 'recovery' level, with a certain refractory period. The synapses are modeled as a variable conductance with a battery potential. For each spike, after a specified delay (corresponding to the sum of possible axonal, neurotransmitter, and dendritic delays), the conductance will increase by a set 'weight' and then exponentially decay. The post-synaptic membrane potential is thus pulled towards the specified battery potential for that synapse, with a strength corresponding to the conductance. The synaptic weights can also undergo short-term depression or facilitation, so that successive spikes may have a lesser or greater effect in changing the post-synaptic membrane potential.

These elements are used in a simulated neural circuit that closely resembles that of the cricket as illustrated in Fig. 5B. The input to the left and right auditory interneurons is represented by eight 'parallel fibers' from the ear sensors, which encode the sound in Poisson distributed spike trains proportional to the amplitude. One pair of auditory interneurons (ON1) provide cross-inhibition, the other pair (AN1) connects to the 'brain' neurons (BNC1 and BNC2).

Our initial aim was to copy the response patterns reported for brain neurons in the cricket by Schildberger in 1984 (see above). This required us to flesh out the specific mechanisms by which high-pass, low-pass or band-pass properties might be obtained. However, it was impossible to tune neuron or synapse parameters to produce a high-pass neural response that could distinguish very slow rates from very fast rates. Fast rates (which have short gaps between syllables) are not clearly coded by either the real or the simulated AN1 neurons, so the response to a chirp made up of many short syllables at a fast rate closely resembles the continuous firing seen during a long syllable at a slow rate. In other words, at the upper limit, a fast rate is a continuous sound, and at the lower limit, a slow rate is a continuous sound. Hence any 'high-pass' mechanism that could filter

out slow rates would also filter out fast rates, making it already a band-pass filter. We found that a low-pass filter could be produced by having a moderately depressing synaptic connection from AN1 to BNC1. This would fire several spikes at the onset of syllables. If the syllables and gaps were short, the depression would not recover and fewer spikes would occur. For longer syllables and gaps, the recovery would be greater and the chance of spiking at syllable onsets increased; but the time between onsets also increased. Thus the total number of spikes within a fixed duration (the spike rate) decreased. There was a second depressing synaptic connection from BNC1 to BNC2, with BNC2 using a relatively slow time constant to perform temporal summation of the BN1 output. The slower rates fail to summate, making BNC2 a band-pass filter for the correct syllable rate. The output of BNC2 is a spike, approximately once per chirp, if the sound pattern has the correct syllable rate, on the side corresponding to the loudest sound, indicating a turn in that direction is needed to approach the calling song.

3.2.3. Motor control

As already discussed, there is little specific neurophysiological information about the output circuitry involved in phonotaxis. The available behavioral data suggested that the cricket usually moves in short bursts of forward walking, with turns in response to sound occurring every couple of seconds, both during walking and after stopping. (Although more recent data suggests that in fact small directional adjustments happen more often, possibly in response to individual syllables in the song—Hedwig and Poulet, personal communication). We devised a simple simulated neural circuit to control the robot's movement in a similar manner (Fig. 7). The paired burst generators (BG) will, when initiated by an incoming spike, mutually activate each other to produce a continuous burst of spikes that go to right and left forward neurons (RF and LF) and drive the robot forward. The length of the burst is limited by the eventual activation of the STOP neuron, by input from the BG neurons, which in turn inhibits the BG neurons. One trigger for movement is a spike in the left or right BNC2, indicating a conspecific song detected to the left or right. These also act via a right or left turn neuron (RT or LT) to modulate the forward velocity by appropriate excitatory and inhibitory connections to RF and LF. The burst can also be initiated via a 'go' neuron (GO), which can be used to modulate the overall speed, for example, making the robot move more rapidly in the light.

This control has been tested on three different robot platforms: a small wheeled platform that is similar in size, speed and turning rate to a cricket (Fig. 7B), a larger wheeled platform (that allowed us to incorporate an additional visual sensor, see below), and a biologically inspired 'whegs' platform that mimics six-legged walking (see Ritzmann, Quinn and Fischer, this issue) that was capable of being tested on outdoor terrain. For the two-wheeled platforms, the right forward and left forward neurons could be used directly to control the speed of the motors on the respective sides. For the whegs platform it was necessary to convert the difference in the speeds to a steering signal. In each case the behavior of the robot could be tracked, using either dead-reckoning from the robot's wheel encoders, an overhead camera, or triangulation based on a retractable tether system.

3.3. Results

The various versions of the robot system have undergone a variety of tests under a variety of conditions: further details can be found in Lund et al., 1997; Webb and Scutt, 2000; Reeve and Webb, 2003; Horchler et al., 2003. Here we present a selection of these results to illustrate how the robot can be used to test hypotheses about the cricket's auditory localization capabilities.

The morphology of the auditory system—which limits the range of frequencies for which accurate directional information is available—may contribute to the apparent selectivity of female crickets for a particular carrier frequency in the song. When two simultaneous songs with the correct temporal pattern, but different carrier frequencies are presented, the robot consistently 'prefers' the 4.7 kHz song, although it has no explicit filtering for the sound frequency (Fig. 8). Note that when the robot is tested with two simultaneous songs of the correct carrier frequency, it approaches one or the other, with no particular preference. It does not get confused and move between the songs because of the inherent feedback loop via the robot's behavior: if it turns slightly more towards one sound source, the relative contribution of that source to its next turn will be greater, and thus one sound source will 'capture' the track.

Fig. 9 illustrates the tuning for different syllable rates that results from the neural circuit described in Section 3.2.2. when tested with song patterns identical to those used by Schildberger (1984), i.e. using equal length chirps with syllable repetition intervals (SRI) ranging from 10 to 90 ms. It can be seen that BNC1 has a moderately band-pass response which is sharpened by BNC2. The response of BNC2 is very similar to the BNC2a neuron in the cricket. In the upper plots which show results with artificial square-wave activation of the auditory nerve at different amplitudes, the apparent best tuning is to an SRI of 26 ms. However, using the same neural parameters with real sound signals played to the robot from different distances, as shown in the lower plots, the natural addition of noise means that syllables at this rate are not so clearly coded, and the best response in BNC2 moves to an SRI of between 42 and 58 ms.

The need for a pattern with the correct syllable rate makes the BN2 neurons much more likely to respond if this pattern is clearly represented in AN1, which generally corresponds to the louder side, particularly after the cross-inhibitory effects of ON1. We found it was not necessary to

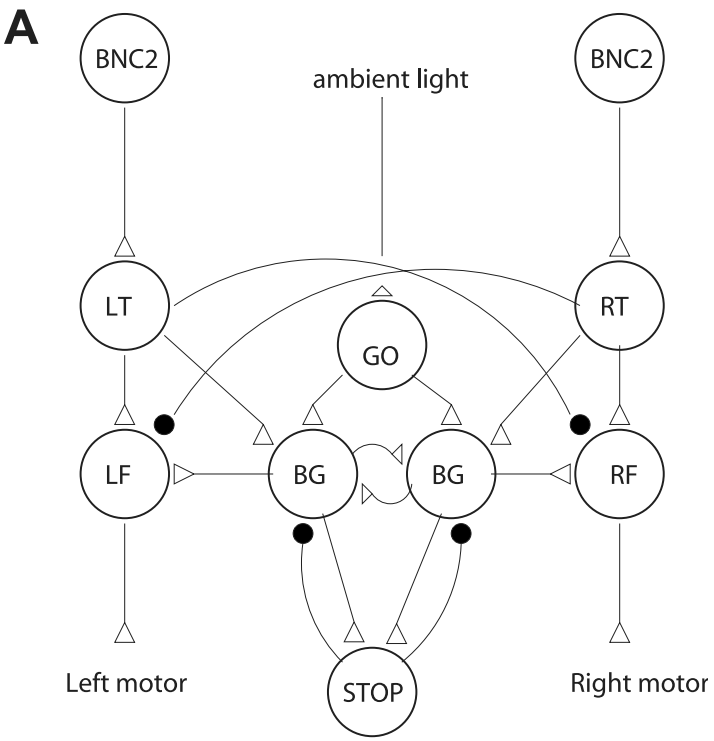

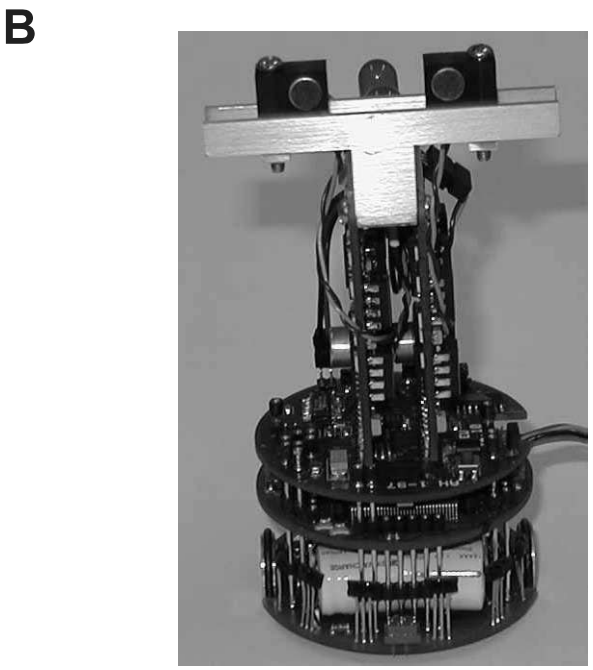

Fig. 7. A. The simulated neural circuit controlling the motor output of the robot (see text for details). B. The small wheeled robot used in experiments. It has a diameter of 5.5 cm.

include any explicit mechanism for comparing the firing rates or latencies at the BNC level. We could simply take a spike in the left or right BNC2 as indicating the need to turn in that direction to approach the sound. The resulting behavior of the robot when tracking the correct sound is shown for three different starting positions in Fig. 10A. The system was tested in the normal lab environment without any soundproofing or control of echoes and background noise, and could reliably locate the speaker producing a cricket song.

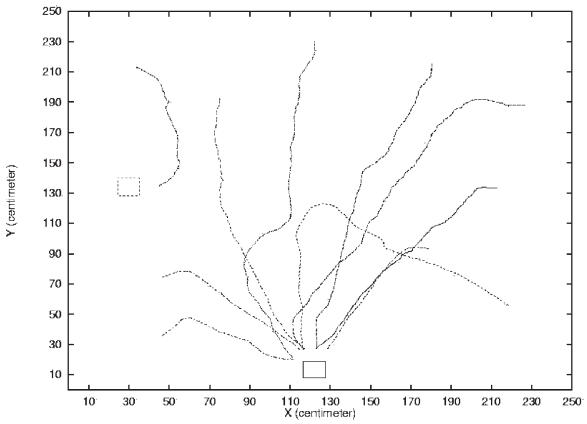

Fig. 8. The behavior of the robot when played two simultaneous calling songs with different carrier frequencies. The lower box is a speaker playing a 4.7 kHz song, which matches the time delays used in the peripheral auditory processing. The left box is a speaker playing a 6.7 kHz song. Each line is a separate trial, with the robot starting from 10 different positions in the arena. It always successfully approaches a sound source; only once is this the song with the wrong carrier frequency.

Fig. 10B shows the behavior when the same neural circuit was used to control the whegs robot in tests in an outdoor environment (a grassy area on the University campus). It can be seen that it is still capable of producing successful localization under these more natural auditory conditions (see Webb et al., 2003 for further discussion of the outdoor results).

4. Combining auditory and visual systems

4.1. Background

Böhm et al. (1991) investigated the interaction between cricket phonotaxis (sound-localizing) behavior and the cricket's response to visual stimuli, including the optomotor response. The results led them to conclude that the 'turning tendency [of the cricket to both stimuli] can be explained as the weighted sum of the turning tendencies evoked by the two individual stimuli'. It seemed straightforward, therefore, to combine the optomotor sensor described in Section 2.2.2 with the phonotaxis system described in Section 3.2, and use a weighted sum of their outputs to control the robot's response. However, we found (Webb and Harrison, 2000a) that the optomotor response tended to interfere with the phonotaxis behavior. Essentially the problem was that each turn towards the sound would produce a clear optomotor stimulus, which would cause the robot to correct itself and turn away from the sound again. This unsatisfactory result was an empirical demonstration of the problem theoretically formulated by von Holst and Mittelstaedt (1950): how can an animal with an optomotor reflex make intentional turns without automatically correcting (and thus negating) them? This problem was not encountered by the crickets in Böhm et al. (1991) study because their behavior was measured under open-loop conditions, which would not produce the normal visual feedback.

One obvious and easily implemented solution to this problem is to have the turning response to sound inhibit the optomotor response, by setting its weighting in the sum temporarily to zero. This kind of switching behavior has been shown in several animal systems, e.g. in response to escape signals in the locust (Robert and Rowell, 1992) and during pursuit turns in the housefly (Srinivasan and Bernard, 1977). Nevertheless there are alternative schemes, which also have some biological support. Collett (1980b) describes several. One is to use 'efferent copy', with the expected optomotor signal resulting from a turn subtracted from the actual signal. Another is 'follow-on', in which the intended turn is actually controlled via the optomotor response by injecting the inverse of the expected signal, so that the optomotor system in correcting for the injected signal executes the desired turn. A third, is to modify the 'additive' scheme so that the size of intended turns is increased to compensate for the expected optomotor feedback.

As Collett (1980b) shows, these three schemes algorithmically all reduce to addition of the two signals with appropriate gains. This implies that our original (additive) system might have worked if we had simply scaled the weighting of phonotaxis to compensate for the optomotor feedback. However as Collett also shows, the schemes are not equivalent when considered at the more detailed level of the temporal dynamics of the different reflexes. This was demonstrated by the fact that we could not find suitable additive gain parameters for the robot. The schemes also differ in their biological plausibility. In fact consideration of possible neural circuits to implement the different schemes results in a less clear distinction between the various options (discussed in detail below).

4.2. Designs

The optomotor and auditory hardware were the same as those used in the previous sections. Both were mounted on a wheeled robot base.

In the initial experiments (described in detail in Webb and Harrison, 2000b) the optomotor signal was used to modulate the motor speeds in a manner directly comparable to the previous optomotor implementation, i.e. the low-pass filtered output of the analog VLSI sensor was added to the left and subtracted from the right motor command sent to the robot wheels. However its influence was gated by the output from the simulated neural circuit that controlled phonotaxis, inhibiting any optomotor response for the duration of each turn triggered towards the sound.

We then considered a neural implementation of the interaction (described in detail in Webb and Reeve, 2003). In this case, the optomotor sensor is used to produce four spike trains, two for each direction of motion. These are summed in two optomotor interneurons, OA and OC, which

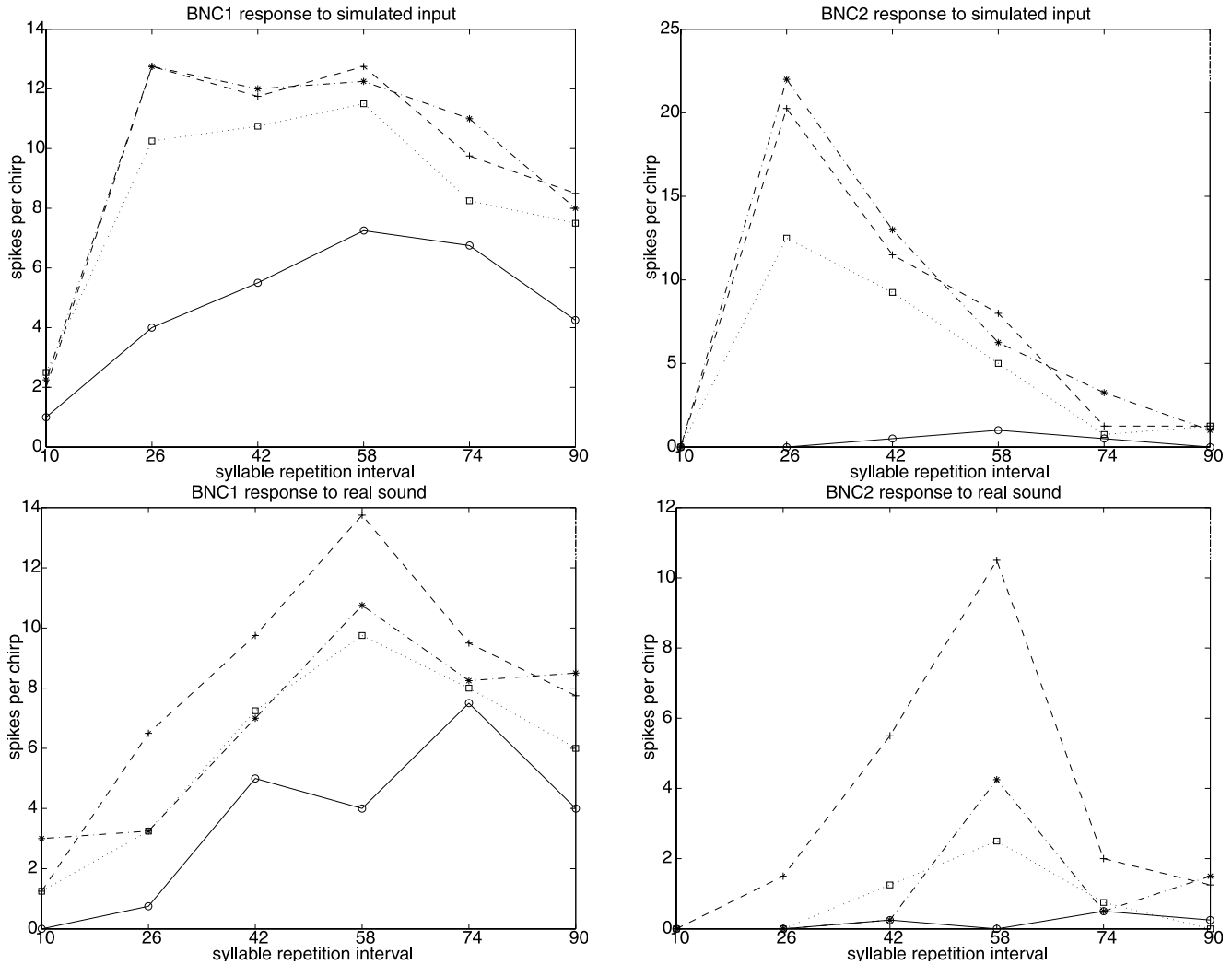

Fig. 9. The activity of the simulated BNC neurons to different syllable repetition intervals. The upper plots are the response when the simulated auditory nerve is stimulated directly with a square wave signal. The lower plots are the response for real sounds in a normal environment. The different line styles represent different amplitudes of the signal: square is the maximum, and the circle, cross and star represent, respectively, 75%, 50% and 25% of the maximum. BNC1 (left) shows a low-pass response and BNC2 a more sharply tuned bandpass. The preferred rate is slightly slower for the real sound.

act as a temporal integration stage. The interneurons mutually inhibit one another. The output from the interneurons steers the robot in the appropriate direction by excitatory inputs to the left or right 'forward' neurons, e.g. leftward visual rotation will result in leftward rotation of the robot.

As described so far, this corresponds to an additive scheme of integration, with the output from the motor neurons being a sum of the inputs from the auditory and the optomotor processing circuits. The obvious way to convert this to an inhibitory scheme is to add inhibitory synaptic connections between the phonotaxis interneuron and the optomotor interneuron corresponding to the expected turn direction, as shown in Fig. 11. This, however, is not precisely the same as the previous inhibition scheme, which would require blocking of all output from both optomotor neurons by the phonotaxis output. Instead, we are using direction specific connections. Also, recall that our synaptic model is conductance based so an inhibitory synapse pulls the membrane potential of the post-synaptic neuron towards a specified battery potential (in this case, the membrane resting level) with a certain conductance strength (i.e. this implements shunting inhibition). Thus it counteracts any optomotor excitation up to the strength of the inhibition. This means the robot might still respond to optomotor signals during a phonotactic turn if the signal is in the opposite direction to that expected, or is much larger than expected. Consequently this scheme also has some of the character of efferent copy.

It is worth noting that it is hard to determine how *precise* efferent copy could be implemented in a simple neural circuit. In theory, to produce the correct cancellation, it would be necessary for the system to be able to predict the

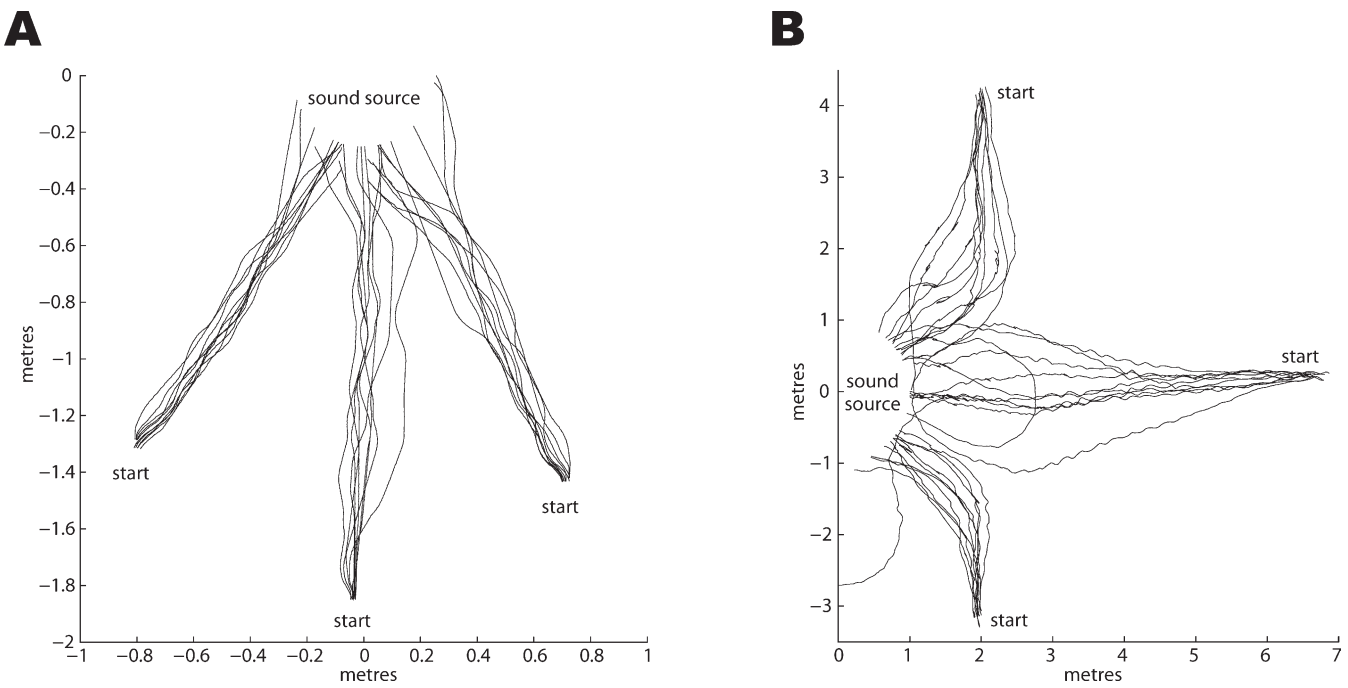

Fig. 10. Tracks of the robot to a cricket song played through a speaker. A. Thirty trials in an indoor environment. B. Thirty trials in an outdoor environment.

exact size and time-course of the expected optomotor signal. As this signal is dependent on the exact turning behaviour, the spatial frequency and contrast of the scene, and the properties of the sensor, these would all have to be predicted, implying the existence of a complete internal 'forward model' of the motor system, environment and sensory system (Webb, 2004). Obviously it is not viable to implement such a model with a few simple neural connections.

4.3. Results

Using the first algorithmic solution, we carried out a series of trials to see whether phonotaxis behavior was improved by the addition of an optomotor reflex (Fig. 12). When we added a constant bias to the robot's movement, to emulate motor asymmetries seen in real crickets, tracking was significantly worse when performed by phonotaxis only. Adding the optomotor response enabled the robot to compensate almost completely for the motor bias and track normally.

Fig. 13 shows the results using the neural implementation. In this case, the robot was tracking the sound source under conditions where random turns were added to the path, to mimic the effects of uneven terrain. It can be seen that incorporating the optomotor reflex as described allows the robot to correct for these deviations and directly approach the sound.

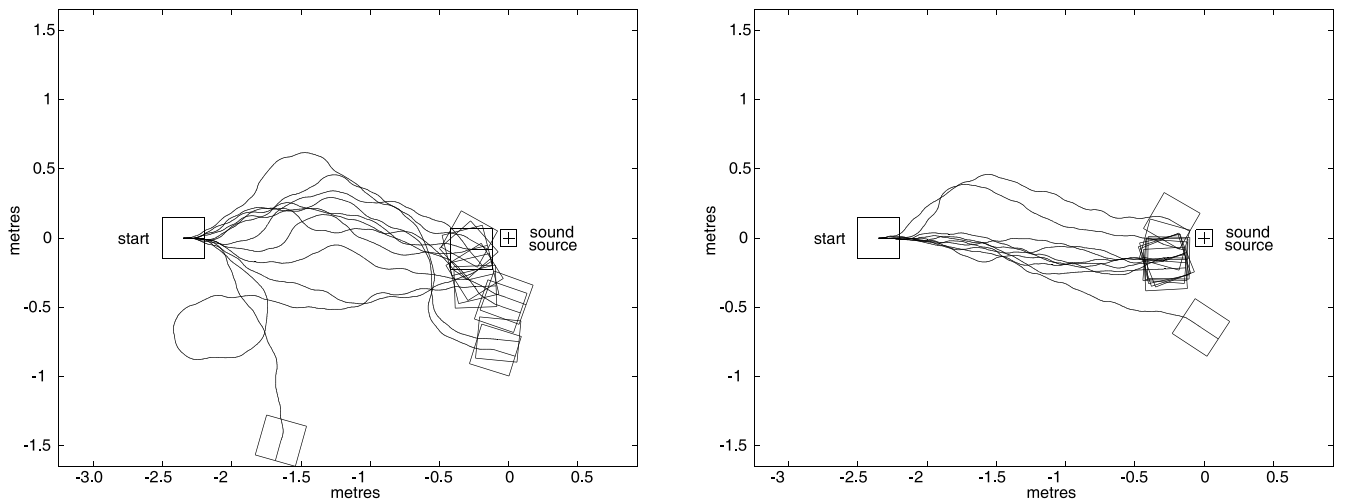

Fig. 11. Tracks of the robot to a cricket song when it has an imposed bias to rightward motion. Left, phonotaxis alone is not always sufficient to overcome the bias and the robot misses the sound source. Right, with an optomotor system also active, the robot is able to track more directly to the sound source.

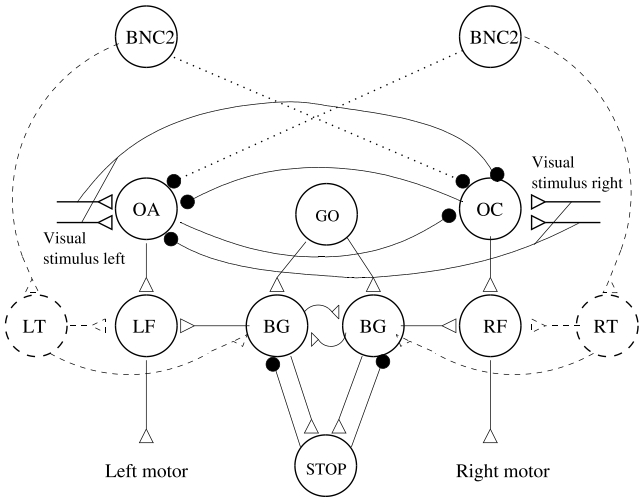

Fig. 12. The simulated neural circuit used to combine the phonotaxis and optomotor systems. The signal from the optomotor chip is integrated in two neurons (OA and OC) and excites the respective forward neurons to compensate for visual rotation. The signal for a phonotactic turn response (BNC2) inhibits the activity of the optomotor neurons for the direction of visual input that is expected to occur during the turn. (Note that the RT/LT connections to the opposite LF/RF neurons, shown in Fig. 11, have been omitted from this figure for legibility).

5. Olfactory-guided navigation

5.1. Background

5.1.1. Behavior

One of the most studied flying odor tracking systems is that of male moths tracking female sex attractant pheromone to locate mates (Arbas et al., 1993; Cardé and Minks, 1997). A typical behavioral response of the moth to detecting odor while flying or walking is to re-orient the direction of locomotion into the wind and to begin moving upwind (Arbas et al., 1993; Bell and Kramer, 1979; Kennedy, 1940). In doing so, visually detected flow field feedback provides information on wind speed and direction that also determines the steering movements (David, 1986; Olberg, 1983). In all flying moths studied thus far (Willis and Arbas, 1997) and many of the walking insects (Bell and Tobin, 1982) an internally generated program of counterturns is also activated upon detection of an attractive odor. It is the combination of these two primary mechanisms that result in the zigzagging upwind paths that we observe from animals tracking windborne plumes of attractive odors (Arbas et al., 1993) (Fig. 14).

To appreciate why this task requires the integration of chemical, air flow, and visual information, plus internally generated turning, it is critical to appreciate the environmental constraints on olfactory orientation. In the previous example of audition, localization was possible by steering until two bilateral sensors are equally stimulated: a process known as tropotaxis (Frankel and Gunn, 1961; Schöne, 1984). This works when the stimulus energy forms a continuous gradient from its source, and the sensors are sufficiently separated to detect it. However, stable concentration gradients of chemical stimuli typically occur only at environmental scales appropriate for use by microscopic organisms such as bacteria and protozoans (Bell and Tobin, 1982; Schöne, 1984). For most other environments and organisms, chemicals evaporating from or actively emitted

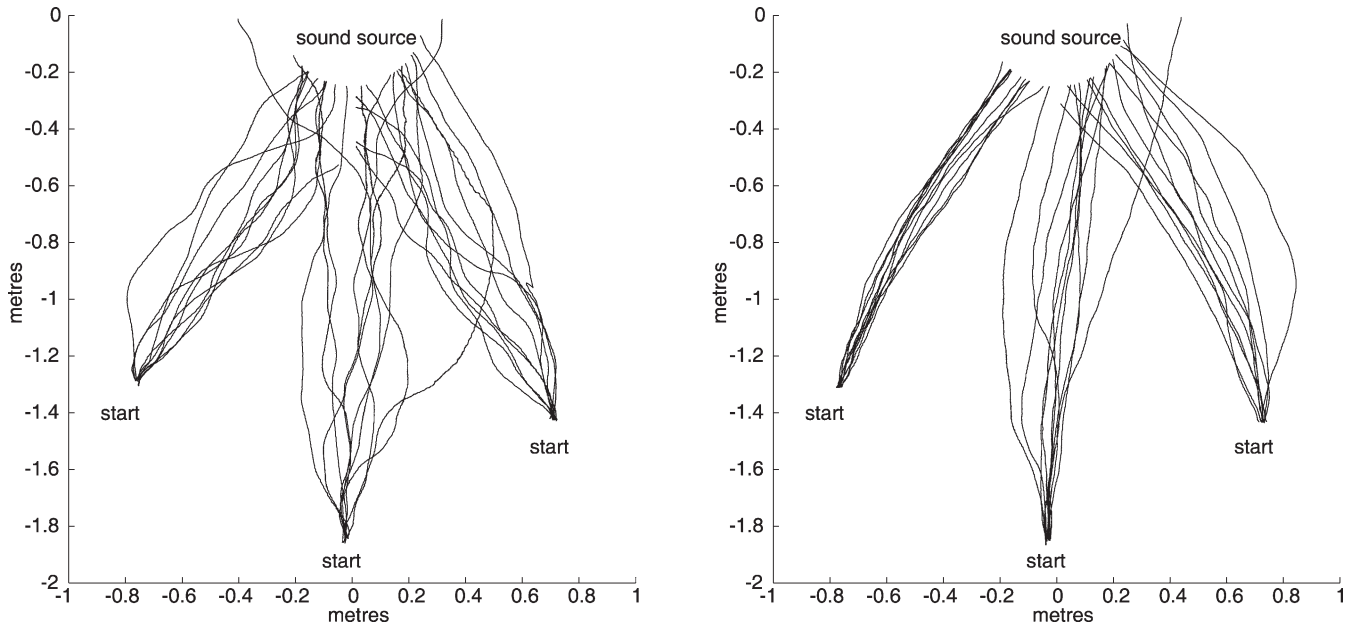

Fig. 13. Tracks of the robot to cricket song when it has an imposed random turn behaviour. Left, phonotaxis alone is not always sufficient for the robot to reach the sound source. Right, with the optomotor signal integrated as shown in Fig. 10, the robot is able to track more directly to the sound source.

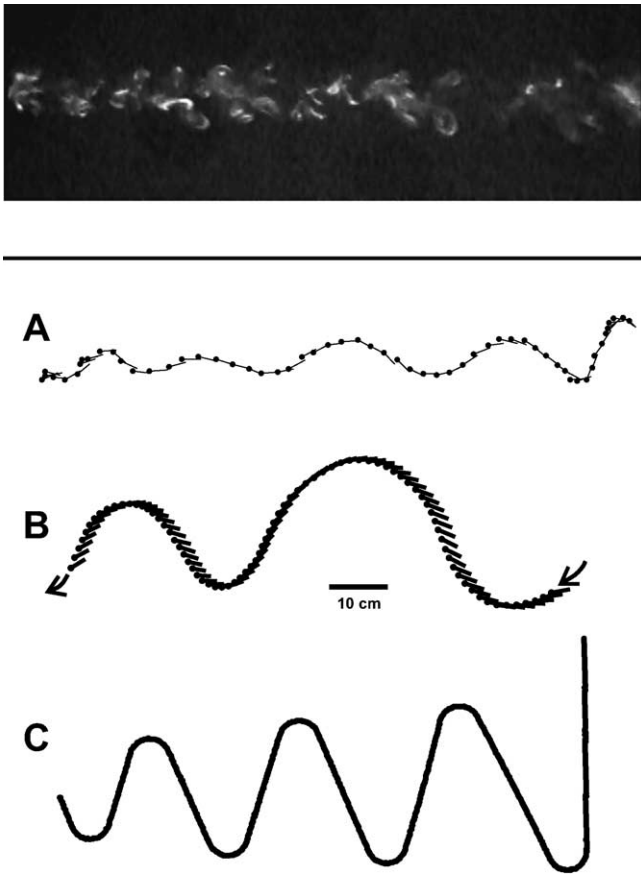

Fig. 14. Top—Image of a smoke plume flow visualization illustrating the intermittent distribution of odorant molecules in wind. In this image, the wind is blowing from left to right. Bottom—Plume tracking responses of a walking cockroach (A), a flying moth (B), and a wheeled robot (C). These three tracks were all generated in the same wind tunnel environment. In this figure the wind blows from left to right.

by a source are borne away in fluid flows (either water or air) of varying turbulence (Fig. 14). Because of the nature of turbulent diffusion (Murlis et al., 1992) a gradient of stimulus intensity cannot form. Turbulent eddies, characterizing the specific flow conditions or generated by the fluid flowing around the chemical source, carry the chemicals away from the source in discrete packets separated by parcels of clean fluid (i.e. air or water). Thus, in most cases an animal orienting toward a source of attractive chemicals experiences the chemical as an intermittent stimulus (airborne: Murlis et al., 1992; waterborne: Weissburg, 2000).

The relevant chemical sensors for male moths tracking plumes of female pheromone are their two antennae. It is thought that they are positioned too closely together, compared to the distances between odor packets in plumes, for bilateral asymmetry between their responses to provide reliable directional information. In many insects the distance separating the two sensors is typically less than 0.5 cm (in one of the more studied species of odor-tracking moth (*Grapholita molesta*: Baker, 1985), the overall length of the moth's body is ca. 5 mm with a full wingspan of ca. 1 cm). Additionally, male moths with one antenna surgically removed have been shown to track a pheromone plume immediately after surgery (Kennedy and Marsh, 1974; Vickers and Baker, 1991; Willis, unpublished observation) with no obvious change in behavior. In contrast, cockroaches, *Periplaneta americana*, appear to be able to scan large volumes of air with their long antennae and detect where in space their antennae encounter pheromone (Hösl, 1990; Heinbockel and Hildebrand, 1998). Upon removal of one antenna the animals generate 'circus movements' turning continuously in the direction of the remaining antenna (Rust et al., 1976) although after two days these animals are able to orient and walk upwind, suggesting a switch from using primarily spatial information to primarily temporal comparisons. Another walking odor-tracking arthropod, the American lobster, *Homarus americanus* shows a similar response to unilateral removal of one of the medial antennules (the odor detecting part of the first antenna), i.e. becoming disoriented and often turning in the direction of the single intact antennule when attempting to track a plume (Beglane et al., 1997).

Flying odor trackers are also typically moving fast relative to the stimulus they are tracking. In the laboratory the wind may carry the plume downwind at ca. 100 cm/s wind speed while the moths are flying upwind at ca. 130–200 cm/s (Arbas et al., 1993; Willis and Arbas, 1997) and males are observed to fly upwind even faster in field studies (Willis et al., 1991; Vickers and Baker, 1997). Approximate calculations based on the width of the pheromone plume together with the wind speed and structure of the flight tracks of male moths, *Manduca sexta*, indicate that males may spend as little as 100 ms traversing the plume. Assuming roughly 100–250 ms for all neural events from sensory transduction to motor activation to occur, and considering that the average time between turns is ca. 500–600 ms during odor tracking flight, it is difficult to imagine that these moths are generating turning maneuvers in response to individual odor onsets and offsets (Belanger and Willis, 1996). Rather, the rapid encounter and loss of odor contact resulting from the constraints of upwind flight combined with the relatively slow sensory transduction processes underlying olfaction (Restrepo et al., 1995) seems to have resulted in the evolution of the pre-programmed steering responses we observe. These behaviors are thought to be pre-programmed and stored in the CNS because they are performed by naïve individuals upon their initial encounter with an odor plume (Bell and Tobin, 1982; Schöne, 1984).

Thus, the physical constraints of chemical (odor) distribution in turbulent flows through complex natural environments, together with the typical size of the agents tracking odor plumes strongly suggest that odor-triggered steering responses in moths are elicited either by the immediate contact or loss with the intermittent odor plume or by temporal comparisons between different locations in

the plume, and not by instantaneous spatial comparisons between bilateral sensors. Behavioral evidence arguing for both of these possibilities exists (modulation of instantaneous internal program—Vickers and Baker, 1992, 1994; Mara-Neto and Cardé, 1994) (temporal comparison along the plume—Kuenen and Baker, 1983; Kennedy, 1983; Willis and Baker, 1994; Willis and Arbas, 1997). It is certainly possible, if not expected, that multiple steering mechanisms could be used and would be supported by the same stream of olfactory information (Frankel and Gunn, 1961; Schöne, 1984). An animal using temporal comparisons to modulate its orientation would also require some sort of short-term memory of at least the previous few seconds. It should not be surprising that any animal possesses and uses this sort of memory, and there is abundant evidence that insects learn and remember information acquired via their olfactory senses (Menzel, 2001; Daly and Smith, 2000).

By extending laboratory studies of odor plume structures and behavior into natural field environments (Elkinton et al., 1984, 1987) two important results have been realized. First, turbulent diffusion generates a pheromone plume which has supra-threshold odor concentrations projecting much further downwind (Elkinton et al., 1984) than predicted by diffusion-based models (Sutton, 1953). Second, even evolved biological systems encounter conditions in their natural environments that are so challenging that the probability of successfully completing the odor tracking task (at least while flying) can be very low (e.g. $<10\%$) (Elkinton et al., 1987).

5.1.2. Anatomy and physiology

As with the other examples of sensory systems presented here, insect olfactory systems are specialized to respond only to specific sub-components of the available information. Many of the known olfactory sensory neurons seem to be tuned to respond to specific molecules (Hildebrand and Shepherd, 1997) and thus may be considered as matched filters. The specificity of response is a continuum ranging from the ultimate in specificity, pheromone receptor neurons responding to the presence of only a single type of odorant molecule, to more broadly tuned receptor neurons responding to general odorants such as food. These general odorant receptors may also respond to only one odorant molecule or, more typically, respond to small groups of molecules with similar structures (e.g. similar length of carbon chain, functional group, or number and site of double bonds) (Shields and Hildebrand, 2001). Much more is known about structure and function of the first processing point for olfactory information in the central nervous system, the antennal lobes (Hildebrand, 1997; Hansson, 2002), where the olfactory receptor neurons on the antennae make their synaptic connections with the central nervous system.

These bilaterally symmetrical structures are made up of arrays of 50–100 characteristically globular structures known as glomeruli (Hildebrand, 1997; Hansson, 2002). Recent studies using the fruit fly *Drosophila melanogaster* have demonstrated receptor neurons expressing specific receptor proteins converging and innervating a specific glomerulus (Gao et al., 2000; Voshall et al., 2000), substantiating anatomical and physiological observations of pheromone sensitive receptors in moths and their specialized pheromone processing glomeruli (Hansson et al., 1992). Activity-dependent recordings in honey bees (Galizia et al., 1998) and moths (Carlsson et al., 2003; Hansson et al., 2003) have now shown that stimulating with even a single type of odorant molecule activates multiple glomeruli in a stereotyped pattern, suggesting that the array of glomeruli may encode the important structural characteristics of the molecules.

Physiological recordings made from the neurons projecting from the antennal lobes to centers in the brain, have revealed an array of cells carrying information, in parallel, on different aspects of the olfactory signal (Christensen et al., 1995; Lei et al., 2001; Muller et al., 2002; Heinbockel et al., 1999; Kanzaki et al., 1991, 2003). These projection neurons carry information on the concentration of individual odorants, blends of specific odorants (i.e. pheromones) (Hansson et al., 1992), and the temporal patterns of odor onset and offset in plumes (Vickers et al., 2001). The specific parts of the brain in which these projection neurons synapse and the function of these destinations in olfactory information processing are only now beginning to be realized. However, the relatively 'raw' odor information carried by these projection neurons will come under higher-order processing, be integrated with other sensory modalities and used in decisions on what behavior to elaborate. It is known that projections from the antennal lobes synapse in the learning and pre-motor areas known as the mushroom bodies (Strausfeld et al., 1998), the lateral accessory lobes of the central body complex (Kanzaki et al., 1991, 2003), and the inferior lateral protocerebrum (Lei et al., 2001; Kanzaki et al., 1991, 2003). However, the functional importance of these different processing areas, how they relate to each other, and the subsequent behavior expressed by the whole organism has only begun to be resolved.

Insects orienting to wind while walking appear to use the mechanical deflection of their antennae to detect the direction and magnitude of the flow they are moving through (Bell and Kramer, 1979). Thus, in these cases the antennae are providing information on both the presence (and absence) of odor and the direction of the flow. Flying insects also use mechanosensory deflection of their antennae (Arbas, 1986; Gewecke, 1977; Gewecke and Niehaus, 1981; Niehaus, 1981), in addition to deflection of mechanosensory hairs on their faces, to detect their speed and direction of movement through the air (Arbas, 1986).

In both walking and flying animals the orientation to flow direction (anemotaxis in air; rheotaxis in water) is typically modulated by odor (Kennedy, 1940; Kennedy and Moorehouse, 1969; Weissburg, 2000; Kennedy and Marsh, 1974;

Arbas et al., 1993). The properties of many of the neurons in the sensory and pre-motor areas of the brains of odor tracking animals are affected by the detection of an attractive odor. Such changes have been recorded in descending interneurons carrying multi-sensory information from the brain to the thoracic ganglion in male moths (Olberg and Willis, 1990; Gray and Willis, 2000; Gray et al., 2002). In these cases descending interneurons sensitive to large field visual motion had their firing rates increase dramatically when moving visual flow fields were experienced simultaneously with presentation of pheromone stimulation. This modulation of the response to visual flow fields by odor could be part of a physiological correlate of the odor modulation of orientation to flow.

Due to the complexity and unresolved issues in functional and anatomical circuitry associated with olfactory processing and the integration of odor information with other sensory modalities, we have chosen to take an explicitly behavioral approach to our initial studies with robotic odor trackers. While it would be interesting and informative to use software or hardware models of the antennal lobes as the initial processing of odor information, the quality and response characteristics of synthetic odor detectors are not sufficiently close to their biological counter parts to make this project worthwhile. Therefore our initial goal has been to develop a robust sensorimotor system consisting of pre-programmed turning behavior that is executed upon odor loss, together with tracks steered at angles with respect to the wind direction.

5.2. Designs

5.2.1. Olfactory system

In our robotic odor tracking experiments ionized air was used as the model for odor because the temporal response of the ion detectors is similar to that of our biological models. Ionized air has been used to model pheromone in field dispersion studies and has been demonstrated to form plume structures similar to co-released insect pheromone (Murlis et al., 1990). Furthermore, man-made chemical detectors with temporal responsiveness rapid enough to support odor-modulated locomotion have been, thus far, difficult to produce. Robotic odor tracking systems have been fabricated and tested, but the behavior of the agents has been considerably slowed because of the slow temporal responsiveness of the sensors (Russell et al., 1995; Ishida et al., 1994; Kazadi et al., 2000; Hayes et al., 2002).

One alternative approach to matching the temporal dynamics, sensitivity and specificity of biological odor sensors is the incorporation of surgically detached antennae, e.g. the use of the antennae of the domestic silkworm moth, *Bombyx mori* on a robot by Kuwana et al. (1995a,b). Although this results in an olfactory system orders of magnitude more sensitive and faster than most artificial sensors, the use of living tissue typically results in significant baseline drift and slow and continuous diminution of response as the tissue dies (Kuwana et al., 1995a,b). More recent experiments using insect antennae as biosensors have largely eliminated baseline drift (Schöning et al., 1998; Schütz et al., 2000), but the problem of inconsistencies in responses across individuals and the slow death of the tissue remain. Although this solution was considered for our experiments, the decision to use ionized air as the plume, and ion detectors as the plume sensors resulted in an olfactory system that could be turned on and off with a switch and avoided the problem of continuous degradation of biological tissue once removed from the donor.

The ion detecting antennae were fabricated to match the length of the antennae of the biological model, the hawkmoth *M. sexta*(Fig. 15A), and had a temporal response similar to other ion detecting systems (i.e. 100 s of Hz) (Murlis and Jones, 1981) and well within the range measured from insect antennae (ca. 10–30 Hz for *M. sexta* males, Marion-Poll and Tobin, 1992). The two antennae were separate bilaterally symmetrical circuits whose inputs were initially processed separately as they are in the antennal lobes of insects. The software that read and processed the antennal inputs also displayed the response of the two antennae on the user interface in real time (Fig. 15B). This allowed the user to easily visualize the olfactory inputs and determine when the antennae were receiving asymmetric inputs (e.g. upon entering the plume at an angle into the wind, one of the antennae always lead the other and this was revealed on the user interface).

The initial experiments were aimed at testing very basic algorithms consisting of stereotyped steering responses triggered by the presence or absence of odor. For this reason the olfactory signal that the robot acted upon was simply the average of the two antennal inputs (Belanger and Willis, 1996; Belanger and Arbas, 1998; Willis et al., 2002).

5.2.1.1. Wind-detecting system. Ideally the wind detection system would be biomimetic in nature, with wind direction and speed information derived from the bending or deflection of a mast by the wind, in a manner similar to the transduction mechanism of insect antennae (Bell and Kramer, 1979; Gewecke, 1977). Since no such sensor is commercially available (although custom-built hair sensors for a robot have been used in modeling the wind-mediated escape behavior of crickets by Chapman and Webb, 2001) a differential pressure transducer (SenSym Inc.) was used as wind sensor. The directional sensitivity of this sensor was defined by the orientation of the openings of the input ports. In the final version of the robot, the input ports of the pressure transducer were extended by adding 7 cm long extensions of aluminum tubing whose tips were bent outward so that the input ports were ca. 180° apart (Fig. 15A). This provided a wind direction sensor with a field of view that allowed steering at an angle to the wind direction from ca. 90° to the left of due upwind to 90° to the right. As long as the robot did not steer a downwind course

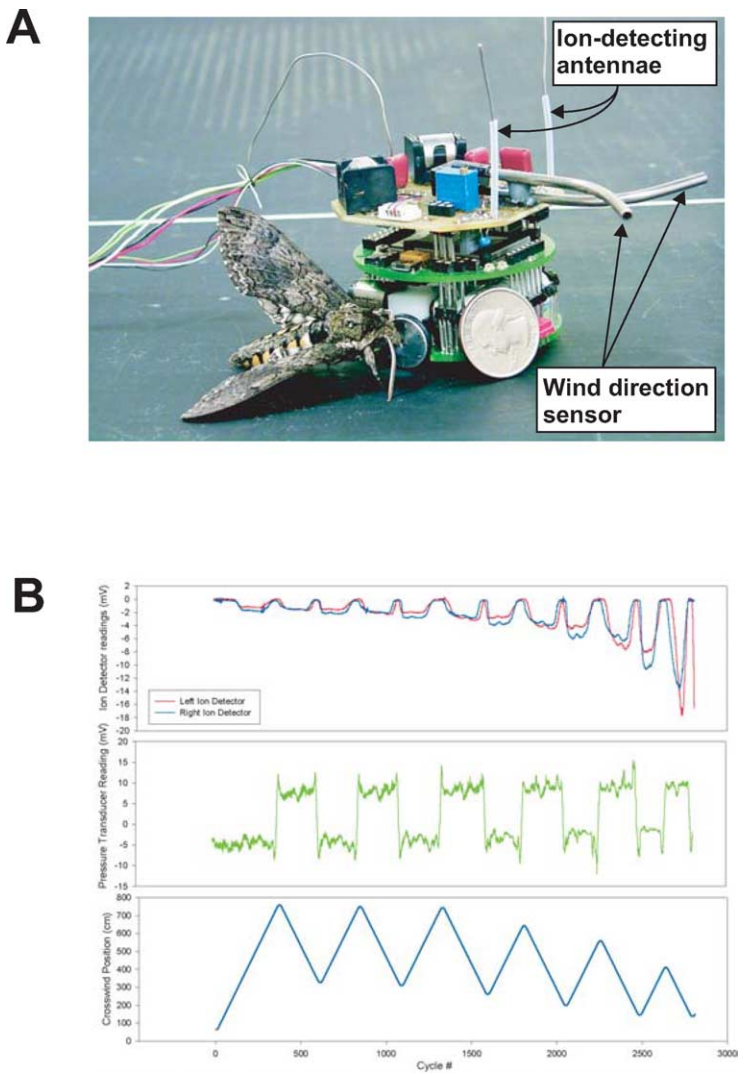

Fig. 15. A. The small wheeled robot with custom fabricated sensory systems parked next to its biological counterpart *Manduca sexta* and a U.S. 25cent coin. B. Antennal and wind sensor (pressure transducer) input and movement track according to wheel encoder readings from a single robot plume tracking trial. Note asymmetric inputs from antennae reflecting the fact that one antenna always leads the other when moving upwind at an angle to the wind. Note also that the ion signal increases as the robot encounters higher ion concentrations close to the source.

the readings from the wind sensor were unambiguous. Further development of this wind sensing system will require either a new sensor, or multiple differential pressure transducers oriented in different directions to remove the ambiguity in the voltage outputs when the robot is aimed in different directions with respect to the wind.

5.2.2. Other sensors and sensor integration

The only other sensors involved in the control of the odor tracking robot were wheel encoders which, in some algorithms, provided the sensory feedback necessary to maintain the orientation of the straight legs between the turns. In all algorithms the encoders provided the sensory feedback necessary for the control of turning behavior. So far we have not incorporated cross-modality modulation of sensory information into our control algorithms. This is primarily because our robot is at an early stage in its development and has so far been specialized to perform a single task. It does not use its sensors to support any behavior other than plume tracking. Thus there is no reason to modulate the gain on the wind detecting sensors the way the visual information appears to be modulated in male moths responding to female pheromone (Olberg and Willis, 1990; Gray et al., 2002).

In one algorithm the magnitude of the turns performed after odor loss were modulated according to the local ion concentration in the plume. But this didn't require the gain on the wheel encoders to change, only for the magnitudes of the turns to be executed according to the local ion concentration. So, even though the algorithm that the robot is performing may be supported by three different sensory modalities (i.e. ion detectors, pressure transducer,

wheel encoders) they are all operating somewhat independently, in large part because of the specialized task that the robot has been designed to perform. It has not yet been called upon to perform any task dependent prioritization of sensory information that would require complex sensor integration.

So far the plume tracking task does not require the integration of steering commands like the auditory tracker with its optomotor stabilization system (see 3.4 above). In the odor tracking robot the loss of odor triggers the performance of pre-programmed fixed magnitude turns that, once initiated, are not performed according to olfactory inputs, in a manner similar to flying and walking odor tracking insects (Arbas et al., 1993; Bell and Tobin, 1982). Thus because of the differences in the physics of the stimuli (i.e. sound vs. odor) and how they interact with the environment the tasks the auditory tracker and odor tracker perform are essentially different and so far the robots require different levels of integration.

5.2.3. Organization of plume tracking behavior

In almost all cases research aimed at the development of robots for odor detection and source location have begun with a primary focus on tracking the plume using only the olfactory system of the robot (Grasso et al., 2000; Ishida et al., 1993; Kuwana et al., 1995a,b; Kazadi et al., 2000; Sandini et al., 1993). However it is generally found that chemotaxis alone yields poor performance (an exception reported by Kazadi et al. (2000) turned out to depend on the unintended property that the odor sensors used were more sensitive when facing upwind). Hence most current odor tracking robot projects incorporate flow sensing of some sort into their robots and control algorithms (Russell et al., 1995; Grasso and Atema, 2002; Hayes et al., 2002; Ishida et al., 1994) which substantially improves the ability to locate the source (Grasso and Atema, 2002; Russell, 1999).

Our wheeled robot was challenged to track ion plumes in the same laboratory wind tunnel used for our insect odor tracking experiments (Willis and Arbas, 1991) using several different control algorithms. All algorithms possessed a plume onset and offset threshold that was variable, and set to result in 'in plume' determinations for the robot at ca. 25 cm on either side of the plume centerline, 1.5 m downwind from the ion source. No obvious change in behavior resulted from the onset of contact with the odor plume. However, in all cases the algorithms were programmed to execute a pre-programmed 'turn back' toward the plume upon loss of odor. The turn magnitude was variable as was the orientation of the straight legs between the turns. These two values could be varied independently and then held constant to test for 'optimal' combinations of turn magnitudes and straight leg orientations for source location. They could also be set to be modulated according to the locally experienced concentration of the plume. The algorithm automatically changed the sign of the turning direction (i.e. 0° = due upwind; 180° = rightward; -180° = leftward) after each turn. The result of these rules was the generation of a zigzagging upwind track similar to those observed from plume tracking animals (Fig. 14B). By initiating the turns upon loss of odor these onset and offset thresholds also determined the lengths of the inter-turn straight legs in the zigzagging track (Fig. 14B). That is, once a turn was completed the robot drove straight along a line oriented at an angle to the wind direction (the bearing angle of the straight leg varied according to the algorithm) and continued until it received an odor offset signal, which triggered the next turn.

Our first set of plume tracking algorithms combined the absence of spatial comparisons thought to underlie the plume tracking performance of flying moths with the pre-programmed turning-back behavior often observed from walking plume trackers (Bell and Tobin, 1982). We did not implement a counterturn generator with a stereotyped inter-turn duration similar to what is thought to underlie the turning behavior of flying plume tracking moths (Arbas et al., 1993). Since the wheeled robot moves so much more slowly than the flying moths, there would have been a severe mismatch between the control algorithm and the behavioral capabilities of the platform.

5.3. Results

Most artificial odor sensors are much slower than biological olfactory systems, typically with cycle times from onset to peak to baseline recovery in the range from seconds to minutes (Hayes et al., 2002; Ishida et al., 1994; Kazadi et al., 2000; Sandini et al., 1993). This has led to many tracking performances taking tens of minutes from start to finish, with most of this time devoted to the sensing cycles of the odor detectors. In one odor tracking robot system, an adaptation of the guidance algorithm to use the dynamically changing phase of the sensors' response to concentration changes rather than the peaks, resulted in dramatic decrease in elapsed time from initiation to source location (Ishida et al., 2002).

Robotic odor tracking papers typically show one or a few movement tracks depicting the robot's behavior or a successful trial ending in source location (Russell et al., 1995). Some calculate performance indices of various kinds while others report the proportion of successful trials (ending in location of the odor source) (Hayes et al., 2002; Grasso and Atema, 2002). Sometimes a partial analysis of the tracking behavior is performed (Grasso and Atema, 2002) and yields some explanations for the successes and failures observed. From an engineering perspective these finer grained behavioral analyses are critical to adapting the robot and algorithms to increase their success and from a biological perspective to learning why a biologically based algorithm fails in certain conditions when the real biological tracker does not. Our robot experiments have been performed and analyzed in a manner similar to that used in biological odor tracking experiments

enabling us to make direct comparisons between the robot and animal performances.

Experiments performed with our wheeled odor tracking robot have aimed at understanding the algorithms underlying plume tracking behavior in flying and walking insects. Initially these results demonstrated that specific combinations of turn size and straight leg bearing angle result in better or poorer success at locating the odor source (Willis et al., 2002). Perhaps it is not a surprise that there is a distinct trade-off between time spent plume tracking and successful source location. Shallow turns (i.e. small turn magnitudes) combined with straight legs oriented more upwind result in rapid upwind tracking performance but the robot enters the 'success zone' (5 cm radius downwind of the ion source) in fewer than 50% of the trials. Algorithms performing sharp turns with large turn magnitudes combined with straight legs oriented at a steeper angle with respect to the wind (i.e. more across the wind) successfully located the source nearly every performance. However, the upwind tracking behavior took many times longer than the faster algorithms. We were able to achieve high success rates and relatively rapid upwind tracking by modulating both the turning magnitude and the steering of the straight legs according to the ion concentration detected in the plume previous to the execution of the maneuvers. In this case turn magnitudes and the bearing angles of straight legs that had been associated with rapid or reliable tracking in earlier experiments were arrayed in look-up tables that were accessed by the algorithm when threshold concentration values were crossed as the robot moved upwind approaching the ion source. There were separate look-up tables for each of four concentration thresholds. The values for turn magnitude and straight leg orientation were chosen randomly from these tables by the algorithm. In all of the three algorithms the navigation paths zigzagged upwind toward the source, with the zigzags getting narrower as the robot approached the source (Fig. 16).

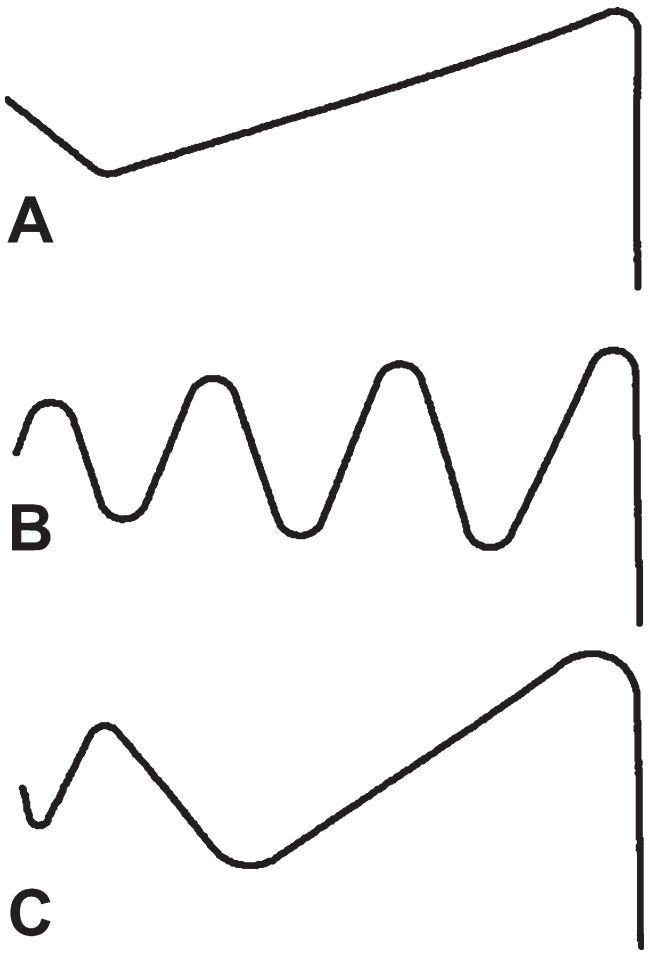

Fig. 16. Examples of robot tracking performances with algorithm settings emphasizing speed to the source, but not source location (A); source location, but not speed to the source (B); and intermediate strategy (C) achieved by modulating the turn magnitude and crosswind steering angle with local plume concentration. Wind in this figure is blowing from left to right.

It is well known that the flight tracks of male moths tracking pheromone plumes get narrower as they approach source (Willis and Arbas, 1991; Charlton et al., 1993; Willis and Baker, 1994). This behavior has been thought to be explained by the modulation of both the optomotor steering and speed control system and the internally generated counterturning generator by predictable changes in the odor plume as the moth approached the source. It is well established that plumes in air and water change in predictable and characteristic ways with distance from the source (Murlis et al., 1990; Moore and Atema, 1991). In our experiments the tracks narrowed as the robot approached the source not because the algorithm was being modulated by the internal structure of the odor plume in a manner similar to that hypothesized for the moths. Rather, the preprogrammed turn-back upon odor loss was initiated sooner for each turn as the robot approached the source because the plume narrowed consistently from the downwind end to the source. So, in a way, even our simplistic tracking algorithm was modulated by predictable changes of the plume as the robot approached the source.

A new type of odor tracking robot designed specifically to test control algorithms of flying plume trackers such as male moths has recently been implemented (Rutkowski et al., 2004). The robot, named 'Robomoth', comprises a suite of sensors (including bilaterally symmetrical ion detectors, a video-based vision system, wind sensors and motor encoders) attached to a three degree of freedom translation system mounted in a wind tunnel. The wind tunnel was constructed to match the dimensions used in the experiments depicted in Fig. 14. Robomoth possesses a complete, albeit simplified, set of the sensors available to the flying odor tracking moths that serve as the biological model for these studies. This new robot will be a major improvement in our ability to test hypotheses on odor-modulated flight control and how inputs from different

sensory modalities affect the processing of other modalities. In addition, Robomoth will be used to address how specific information may be re-prioritized in a task dependent way.

6. Conclusions

Arthropods have received increased levels of interest in recent years because, despite being less complex than larger organisms such as mammals, they are extremely successful in virtually every habitat type on earth. Like the sensory systems of all animals, those of insects serve as filters, detecting only a small subset of the available environmental energy. However, that subset of information is often specific to particular behavioral tasks necessary for their survival and reproduction. In addition, their small size and limited neural processing capabilities has led to highly efficient solutions. Some engineers now actively seek out collaborations with those studying neural control of behavior in arthropods, in search of solutions to difficult problems in robot sensory-motor control. Although the examples presented here show robot capabilities comparable to engineered solutions, as yet it is debatable whether better results will be obtained than by conventional methods. It may turn out that biological solutions are not in fact the most effective ones to adopt for engineering; yet the clear superiority of even 'simple' arthropods to any existing robots suggests this approach is worth continued investigation. In addition, implementing these solutions on robots can be justified by the fact that such implementations can be very informative for biologists.

The work on analog VLSI chips for optomotor and looming detection has translated a set of functions—bandpass filtering, delay, passing through a non-linearity, correlation and opponent subtraction—that are thought to be implemented in the fly visual system. The results show this set of functions is sufficient to account for the optomotor correction behavior seen in the fly, under realistic and noisy stimulus conditions. For cricket phonotaxis, the robot implementation revealed several limitations in the prevailing hypotheses about sound recognition and localization. The two functions could in fact be tightly linked, with carrier frequency filtering a function of the physical structure underlying sound directionality. A new hypothesis was developed that accounts for syllable rate filtering as a function of short-term dynamics of synaptic connections. In combining this behavior with the optomotor system and testing it on the robot, again the existing hypothesis from biology was found to be inadequate, and a range of alternatives were proposed. For olfactory behavior in the moth, the robot allows the exploration of the effects of different parameters such as turn size, and onset and offset thresholds on the performance of plume-following algorithms. These algorithms are then tested in exactly the same experimental situation as the moth. The control of some of these parameters (e.g., turn size and orientation of straight legs) has been largely overlooked by the biologists studying this behavior.

All three examples presented here use robot technology to test biological hypotheses, but it is worth noting some of the differences in these implementations. Some functions have been realized completely in analog hardware, with the advantages of obtaining continuous and rapid processing well matched to the biology. Others combine both hardware and software processing, with the latter implemented either in terms of moderately realistic spiking neurons or in more abstracted control algorithms. An advantage of using software is the greater flexibility in redesigning the control systems and also the relative ease with which all elements of the system can be measured and recorded for later analysis. This is particularly useful if the aim of the model building is to make direct comparisons with the biology, e.g. the spiking rates of known neural elements, or detailed aspects of the flight behavior. It may be less important if the aim is more technological.

It is also interesting to note similarities and differences in the sensorimotor controllers. In each case the behaviors are implemented as rather tight feedback loops, with the robots making continuous adjustments to deviations. This enables them to achieve the target behavior despite noisy input and without requiring precision tuning in the sensory system. Another point of commonality is the principle that sensory processing often seeks to suppress the dc (continuous) input, and enhance the ac (changing) input. An alternative way of considering this is that the system has greater sensitivity to a certain frequency of alternation. In the artificial EMD this is used to enhance the 2–40 Hz range of stimuli, which is the most relevant for detecting visual motion. In the artificial neural circuit for the cricket, short-term adaptation in synapses is used to obtain a band-pass response to syllable rates around 20–40 Hz. In the artificial moth, the tracking behavior depends on reacting to the onset and loss of the plume stimulus.

On the other hand there are clear differences in the behavioral mechanisms needed to make directional responses to the differing kinds of stimuli. The optomotor response provides continuous modulation of the relative left–right speed, the phonotaxis response involving a fixed size of turn in the direction of error, whereas the plume-tracking does not utilize the left–right difference at all, but rather performs pre-programmed turns upon threshold detection of odor loss.

These differences have consequences for the possible interactions of the different behaviors, as well as the integration of incoming sensory information and ongoing behavioral outflow. Such interactions are clearly more complex than vector addition of the directional outputs or winner-take-all selection of the strongest response (two popular current approaches to

the behavioral choice problem in robotics). Animals performing tasks like those discussed above often encounter obstacles that they must negotiate. They are then forced to switch tasks and re-prioritize their sensory inputs from auditory or olfactory to touch, vision or whatever combination necessary to overcome the obstacle. Once the obstacle has been negotiated they must then return to the higher order task (e.g. mate finding). Understanding the control of these so-called transitional behaviors and the often shifting priorities for information from different sensory modalities associated with their successful performance is of major interest to biologists. Successful autonomous robotic vehicles must possess these capabilities to perform in complex real-world environments. Thus, ongoing iterative cycles of animal and robot experiments promise to yield a better understanding of how animals resolve such seemingly conflicting processes in a smooth and efficient manner, as well as providing new ideas for robotic control algorithms. These issues of multimodal integration, in addition to the use of more realistic walking or flying robots to tackle problems of sensory control of more complex motor systems, are promising areas for future collaboration between biological and engineering study.

References

Adelson, E.H., Bergen, J.R., 1985. Spatiotemporal energy models for the perception of motion. Journal of the Optical Society of America A 2, 284–299.

Arbas, E.A., 1986. Control of hindlimb posture by wind-sensitive hairs and antennae during locust flight. Journal of Comparative Physiology A 159, 849–857.

Arbas, E.A., Willis, M.A., Kanzaki, R., 1993. Organization of goal-oriented locomotion: pheromone-modulated flight behavior of moths. In: Beer, R., Ritzmann, R., McKenna, I. (Eds.), Biological Neural Networks in Invertebrate Neuroethology and Robotics.

Autrum, H., 1958. Electrophysiological analysis of the visual systems in insects. Experimental Cell Research Supplement 5, 426–439.

Baker, T.C., 1985. Chemical control of behavior. In: Kerkut, G.A., Gilbert, L.I. (Eds.), Comprehensive Insect Physiology, Biochemistry and Pharmacology, Pergamon Press, Oxford.

Beglane, P.F., Grasso, F.W., Basil, J.A., Atema, J., 1997. Far field chemo-orientation in the American lobster, *Homarus americanus*: effects of unilateral ablation, and lesioning of the lateral antennule. Biological Bulletin 193, 215–215.

Belanger, J.H., Arbas, E.A., 1998. Behavioral strategies underlying pheromone-modulated flight in moths: lessons from simulation studies. Journal of Comparative Physiology A 183, 345–360.

Belanger, J.H., Willis, M.A., 1996. Adaptive control of odor-guided locomotion: behavioral flexibility as an antidote to environmental unpredictability. Adaptive Behavior 4, 217–253.

Bell, W.J., Kramer, E., 1979. Search and anemotactic orientation of cockroaches. Journal of Insect Physiology 25, 631–640.

Bell, W.J., Tobin, T.R., 1982. Chemo-orientation. Biological Review 57, 219–260.

Bennett-Clark, H.C., 1989. Songs and the physics of sound production. In: Huber, F., Moore, T.E., Loher, W. (Eds.), Cricket Behavior and Neurobiology, Cornell University Press, Ithaca, NY, pp. 227–261.

Borst, A., 1990. How do flies land? BioScience 40, 292–299.

Borst, A., Bahde, S., 1988. Visual information processing in the fly's landing system. Journal of Comparative Physiology A 163, 167–173.

Borst, A., Haag, J., 1996. The intrinsic electrophysiological characteristics of fly lobular plate tangential cells: I. Passive membrane properties. Journal of Computational Neuroscience 3, 313–336.

Böhm, H., Schildberger, K., Huber, F., 1991. Visual and acoustic course control in the cricket *Gryllus-bimaculatus*. Journal of Experimental Biology 159, 235–248.

Cardé, R.T., Minks, A.K., 1997. Pheromone Research: New directions, Chapman and Hall, New York.

Carlsson, M.A., Galizia, C.G., Hansson, B.S., 2003. Spatial representation of odours in the antennal lobe of the moth *Spodoptera littoralis* (Lepidoptera: Noctuidae). Chemical Senses 27, 231–244.

Chapman, T., Webb, B., 2001. A robot model of escape and wall-following in cricket and cockroach, Sixth International Congress of Neuroethology.

Charlton, R.E., Kanno, H., Collins, R.D., Cardé, R.T., 1993. Influence of pheromone concentration and ambient temperature on flight of the gypsy moth, *Lymantria dispar* (L), in a sustained-flight wind tunnel. Physiological Entomology 18, 349–362.

Christensen, T.A., Mustaparta, H., Hildebrand, J.G., 1995. Chemical communication in heliothine moths. 6. Parallel pathways of information-processing in the macroglomerular complex of the male tobacco budworm moth *Heliothis virescens*. Journal of Comparative Physiology A 177, 545–557.

Collett, T.S., 1980a. Some operating rules for the optomotor system of a hoverfly during voluntary flight. Journal of Comparative Physiology 138, 271–282.

Collett, T.S., 1980b. Angular tracking and the optomotor response: an analysis of visual reflex interaction in a hoverfly. Journal of Comparative Physiology 140, 145–158.

Daly, K.C., Smith, B.H., 2000. Associative olfactory learning in the moth *Manduca sexta*. Journal of Experimental Biology 203, 2025–2038.

David, C.T., 1986. Mechanisms of directional flight in wind. In: Payne, T.L., Birch, M.C., Kennedy, C.E.J. (Eds.), Mechanisms in Insect Olfaction, Clarendon Press, Oxford, pp. 49–58.

DeVoe, R.D., 1980. Movement sensitivities of cells in the fly's medulla. Journal of Comparative Physiology A 138, 93–119.

DeVoe, R.D., Ockleford, E.M., 1976. Intracellular responses from cells in the medulla of the fly, *Calliphora erythrocephala*. Biological Cybernetics 23, 13–24.

Dong, D.W., Atick, J.J., 1995. Temporal decorrelation: a theory of lagged and nonlagged responses in the lateral geniculate nucleus. Network 6, 159–178.

Dror, R.O., O'Carroll, D.C., Laughlin, S.B., 2001. Accuracy of velocity estimation by Reichardt correlators. Journal of the Optical Society of America A 18, 241–252.

Duchon, A.P., Warren, W.H., Kaelbling, L.P., 1998. Ecological robotics. Adaptive Behavior 6, 473–507.

Egelhaaf, M., 1985. On the neuronal basis of figure-ground discrimination by relative motion in the visual system of the fly: II. Figure-detection cells, a new class of visual interneurones. Biological Cybernetics 52, 195–209.

Egelhaaf, M., 1987. Dynamic properties of two control-systems underlying visually guided turning in house-flies. Journal of Comparative Physiology A 161, 777–783.

Egelhaaf, M., Borst, A., 1989. Transient and steady-state response properties of movement detectors. Journal of the Optical Society of America A 6, 116–127.

Egelhaaf, M., Borst, A., 1993. A look into the cockpit of the fly: visual orientation, algorithms, and identified neurons. Journal of Neuroscience 13, 4563–4574.

Egelhaaf, M., Hausen, K., Reichardt, W., Wehrhahn, C., 1988. Visual

course control in flies relies on neuronal computation of object and background motion. TINS 11, 351–358.
Elkinton, J.S., Cardé, R.T., Mason, C.J., 1984. Evaluation of time-average dispersion models for estimating pheromone concentration in a deciduous forest. Journal of Chemical Ecology 10, 1081–1108.
Elkinton, J.S., Schal, C., Ono, T., Cardé, R.T., 1987. Pheromone puff trajectory and upwind flight of male gypsy moths in a forest. Physiological Entomology 12, 399–406.
Esch, H., Huber, F., Wohlers, D.W., 1980. Primary auditory interneurons in crickets: physiology and central projections. Journal of Comparative Physiology A 137, 27–38.
Franceschini, N., Pichon, J.M., Blanes, C., 1992. From insect vision to robot vision. Philosophical Transactions of the Royal Society of London B 337, 283–294.
Frankel, G.S., Gunn, D.L., 1961. The Orientation of Animals: Kineses, Taxes and Compass Reactions, Dover Publications Inc., New York.
Gabbiani, F., Krapp, H.G., Laurent, G., 1999. Computation of object approach by a wide-field, motion-sensitive neuron. Journal of Neuroscience 19, 1122–1141.
Galizia, C.G., Nagler, K., Holldobler, B., Menzel, R., 1998. Odour coding is bilaterally symmetrical in the antennal lobes of honeybees (*Apis mellifera*). European Journal of Neuroscience 10, 2964–2974.
Gao, Q., Yuan, B., Chess, A., 2000. Convergent projections of *Drosophila* olfactory neurons to specific glomeruli in the antennal lobe. Nature Neuroscience 3, 780–785.
Geiger, G., Nässel, D.R., 1981. Visual orientation behaviour of flies after selective laser beam ablation of interneurones. Nature 293, 398–399.
Geiger, G., Nässel, D.R., 1982. Visual processing of moving single objects and wide-field patterns in flies: behavioural analysis after laser-surgical removal of interneurons. Biological Cybernetics 44, 141–149.
Gewecke, M., 1977. Control of flight in relation to the air in *Locusta migratoria* (Insecta, Orthoptera). Journal of Physiology, Paris 73, 581–592.
Gewecke, M., Niehaus, M., 1981. Flight and flight control by the antennae in the small tortoiseshell (*Aglais urticae* L., Lepidoptera). I. Flight balance experiments. Journal of Comparative Physiology A 145, 249–256.
Götz, K.G., 1975. The optomotor equilibrium of the *Drosophila* navigation system. Journal of Comparative Physiology A 99, 187–210.
Grasso, F.W., Atema, J., 2002. Integration of flow and chemical sensing for guidance of autonomous marine robots in turbulent flows. Journal of Environmental Fluid Mechanics 1, 1–20.
Grasso, F.W., Consi, T.R., Mountain, D.C., Atema, J., 2000. Biomimetic robot lobster performs chemo-orientation in turbulence using a pair of spatially separated sensors: progress and challenges. Robotics and Autonomous Systems 30, 115–131.
Gray, J.R., Willis, M.A., 2000. Neural ensemble recording during active locomotion in virtual reality, Society for Neuroscience, Abstracts 26.
Gray, J.R., Pawlowski, V., Willis, M.A., 2002. A method for recording behavior and multineuronal CNS activity from tethered insects in virtual space. Journal of Neuroscience Methods 120, 211–223.
Haag, J., Borst, A., 1998. Active membrane properties and signal encoding in graded potential neurons. Journal of Neuroscience 18, 7972–7986.
van Hateren, J.H., 1992. Theoretical predictions of spatiotemporal receptive fields of fly LMCs, and experimental validation. Journal of Comparative Physiology A 171, 157–170.
van Hateren, J.H., 1997. Processing of natural time series of intensities by the visual system of the blowfly. Vision Research 37, 3407–3416.
Hansson, B.S., 2002. A bug's smell—research into insect olfaction. Trends in Neurosciences 25, 270–274.
Hansson, B.S., Ljungberg, H., Hallberg, E., Löfstedt, C., 1992. Functional specialization of olfactory glomeruli in a moth. Science 256, 1313–1315.
Hansson, B.S., Carlsson, M.A., Kalinova, B., 2003. Olfactory activation patterns in the antennal lobe of the sphinx moth, *Manduca sexta*. Journal of Comparative Physiology A 189, 301–308.
R.R. Harrison, 2003. A low-power analog VLSI visual collision detector. To appear in Proceedings of NIPS 2003 Conference.
Harrison, R.R., Koch, C., 1999. A robust analog VLSI motion sensor. Autonomous Robots 7, 211–224.
Harrison, R.R., Koch, C., 2000a. A robust analog VLSI Reichardt motion sensor. Analog Integrated Circuits and Signal Processing 24, 213–229.
Harrison, R.R., Koch, C., 2000b. A silicon implementation of the fly's optomotor control system. Neural Computation 12, 2291–2304.
Hassenstein, B., Reichardt, W., 1956. Systemtheoretische Analyse der Zeit-Reihenfolgen-, und Vorzeichenauswertung bei der Bewegungsperzeption des Rüsselkäfers Chlorophanus. Z. Naturforch. 11b, 513–524.
Hausen, K., 1982a. Motion sensitive interneurons in the optomotor system of the fly I. The horizontal cells: structure and signals. Biological Cybernetics 45, 143–156.
Hausen, K., 1982b. Motion sensitive interneurons in the optomotor system of the fly II. The horizontal cells: receptive field organization and response characteristics. Biological Cybernetics 46, 67–79.
Hausen, K., 1984. The lobula-complex of the fly: structure, function, and significance in behaviour. In: Ali, M.A., (Ed.), Photoreception and Vision in Invertebrates, Plenum, New York, NY, pp. 523–559.
Hausen, K., Egelhaaf, M., 1989. Neural mechanisms of visual course control in insects. In: Stavenga, D.G., Hardie, R.C. (Eds.), Facets of Vision, Springer, Berlin.
Hausen, K., Wehrhahn, C., 1990. Neural circuits mediating visual flight control in flies: II. Separation of two control-systems by microsurgical brain-lesions. Journal of Neuroscience 10, 351–360.
Hayes, A.T., Martinoli, A., Goodman, R.M., 2002. Distributed odor source localization. IEEE Sensors Journal 2, 260–271.
Heinbockel, T., Hildebrand, J.G., 1998. Antennal receptive fields of pheromone-responsive projection neurons in the antennal lobes of the male sphinx moth *Manduca sexta*. Journal of Comparative Physiology A 183, 121–133.
Heinbockel, T., Christensen, T.A., Hildebrand, J.G., 1999. Temporal tuning of odor responses in pheromone-responsive projection neurons in the brain of the sphinx moth *Manduca sexta*. Journal of Comparative Neurology 409, 1–12.
Heisenberg, M., Buchner, E., 1977. The role of retinula cell types in visual behaviour of *Drosophila melanogaster*. Journal of Comparative Physiology 117, 127–162.
Hengstenberg, R., 1982. Common visual response properties of giant vertical cells in the lobula plate of the blowfly *Callifora*. Journal of Comparative Physiology A 149, 179–193.
Hildebrand, J.G., 1997. Olfactory control of behavior in moths: central processing of odor information and the functional significance of olfactory glomeruli. Journal of Comparative Physiology A 178, 5–19.
Hildebrand, J.G., Shepherd, G.M., 1997. Molecular mechanisms of olfactory discrimination: converging evidence for common principles across phyla. Annual Review of Neuroscience 20, 593–631.
Holmqvist, M.H., Srinivasan, M.V., 1991. A visually evoked escape response of the housefly. Journal of Comparative Physiology A 169, 451–459.
von Holst, E., Mittelstaedt, H., 1950. Das Reafferenzprinzip, Wechselwirkungen zwischen Zentralnervensystem und Peripherie. Naturwissenschaften 37, 464–476.
Horchler, A.D., Reeve, R.E., Webb, B., Quinn, R.D., 2003. Robot phonotaxis in the wild: a biologically inspired approach to outdoor sound localisation. Advanced Robotics.
Horseman, G., Huber, F., 1994. Sound localisation in crickets II. Modelling the role of a simple neural network in the prothoracic ganglion. Journal of Comparative Physiology A 175, 399–413.
Hösl, M., 1990. Pheromone-sensitive neurons in the deutocerebrum of *Periplaneta americana*: receptive fields on the antenna. Journal of Comparative Physiology A 167, 321–327.
Huber, F., Thorson, J., 1985. Cricket Auditory Communication. Scientific American 253, 47–54.
Ishida, H., Nakamoto, T., Moriizumi, T., 1993. Fundamental study of mobile system for smelling-object localization using plural gas sensors,

Proceedings of the Society for Instrument and Control Engineers, Kanazawa, Japan, pp. 767–768.

Ishida, H., Suetsugu, T., Nakamoto, T., Moriizumi, T., 1994. Study of autonomous mobile sensing system for localization of odor source using gas sensors and anemotactic sensors. Sensors and Actuators A 45, 154–157.

Ishida, H., Nakayama, G., Nakamoto, T., Moriizumi, T., 2002. Controlling a gas/odor plume-tracking robot based on transient responses of gas sensors. Proceedings of the Institute of Electrical and Electronic Engineers, Sensors 2, 1665–1670.

Kanzaki, R., Arbas, E.A., Hildebrand, J.G., 1991. Physiology and morphology of protocerebral olfactory neurons in the male moth *Manduca sexta*. Journal of Comparative Physiology A 168, 281–298.

Kanzaki, R., Soo, K., Seki, Y., Wada, S., 2003. Projections to higher olfactory centers from subdivisions of the antennal lobe macroglomerular complex of the male silkmoth. Chemical Senses 28, 113–130.

Kazadi, S., Goodman, R., Tsikata, D., Green, D., Lin, H., 2000. An autonomous water vapor plume tracking robot using passive resistive polymer sensors. Autonomous Robots 9, 175–188.

Kennedy, J.S., 1983. Zigzagging and casting as a response to wind-borne odor: a review. Physiological Entomology 8, 109–120.

Kennedy, J.S., 1940. The visual responses of flying mosquitoes. Proceedings of the Zoological Society of London A 109, 221–242.

Kennedy, J.S., Marsh, D., 1974. Pheromone regulated anemotaxis in flying moths. Science 184, 999–1001.

Kennedy, J.S., Moorehouse, J.E., 1969. Laboratory observations on locust responses to wind-borne grass odour. Entomologia experimentalis et applicata 12, 487–503.

Kimmerle, B., Egelhaaf, M., Srinivasan, M.V., 1996. Object detection by relative motion in freely flying flies. Naturwissenschaften 83, 380–381.

Kimmerle, B., Warzecha, A.-K., Egelhaaf, M., 1997. Object detection in the fly during simulated translatory flight. Journal of Comparative Physiology A 181, 247–255.

Koch, C., 1999. Biophysics of Computation, Oxford University Press, Oxford.

Krapp, H.G., Hengstenberg, R., 1996. Estimation of self-motion by optic flow processing in single visual interneurons. Nature 384, 463–466.

Kuenen, L.P.S., Baker, T.C., 1983. A non-anemotactic mechanism used in pheromone source location by flying moths. Physiological Entomology 8, 277–289.

Kuwana, Y., Shimoyama, I., Miura, H., 1995a. Steering control of a mobile robot using insect antennae. IEEE/RSJ International Conference on Intelligent Robots and Systems 2, 530–535.

Kuwana, Y., Shimoyama, I., Sayama, Y., Miura, H., 1995b. Synthesis of pheromone oriented emergent behavior of a silkworm moth, Proceedings of the Institute of Electrical and Electronic Engineers International Conference on Robotics and Automation, pp. 556–561.

Land, M.F., 1997. Visual acuity in insects. Annual Review of Entomology 42, 147–177.

Laughlin, S.B., 1994. Matching coding, circuits, cells, and molecules to signals—general principles of retinal design in the fly's eye. Progress in Retinal Eye Research 13, 165–196.

Lei, H., Anton, S., Hansson, B.S., 2001. Olfactory protocerebral pathways processing sex pheromone in the male moth, *Agrotis segetum*. Journal of Comparative Neurology 432, 356–370.

Liu, S.-C., Usseglio-Viretta, A., 2001. Fly-like visuo-motor responses of a robot using aVLSI motion-sensitive chips. Biological Cybernetics 85, 449–457.

Lund, H.H., Webb, B., Hallam, J., 1997. A robot attracted to the cricket species *Gryllus Bimaculatus*, Fourth European Conference on Artificial Life, MIT Press, Cambridge, MA.

Mara-Neto, A., Cardé, R.T., 1994. Fine-scale structure of pheromone plumes modulates upwind orientation of flying male moths. Nature 369, 142.

Marion-Poll, F., Tobin, T.R., 1992. Temporal coding of pheromone pulses and trains in *Manduca sexta*. Journal of Comparative Physiology A 171, 505–512.

Mead, C., 1989. Analog VLSI and Neural Systems, Addison-Wesley, Reading, MA.

Menzel, R., 2001. Behavioral and neural mechanisms of learning and memory as determinants of flower constancy. In: Chittka, L., Thomson, J.D. (Eds.), Cognitive Ecology of Pollination, Cambridge University Press, Cambridge, pp. 21–40.

Michelsen, A., Popov, A.V., Lewis, B., 1994. Physics of directional hearing in the cricket *Gryllus bimaculatus*. Journal of Comparative Physiology A 175, 153–164.

Moini, A., Bouzerdoum, A., Eshraghian, K., Yakovleff, A., Nguyen, X.T., Blanksby, A., Beare, R., Abbott, D., Bogner, R.E., 1997. An insect vision-based motion detection chip. IEEE Journal of Solid-State Circuits 32, 279–284.

Moore, P.A., Atema, J., 1991. Spatial information in the three-dimensional fine structure of an aquatic odor plume. Biological Bulletin 181, 408–418.

Muller, D., Abel, R., Brandt, R., Zöckler, M., Menzel, R., 2002. Differential parallel processing of olfactory information in the honeybee, *Apis mellifera* L. Journal of Comparative Physiology A 188, 359–370.

Murlis, J., Jones, C.D., 1981. Fine scale structure of odour plumes in relation to insect orientation to distant pheromone and other attractant sources. Physiological Entomology 6, 71–86.

Murlis, J., Willis, M.A., Cardé, R.T., 1990. Odor signals: patterns in time and space. In: Døving, K., (Ed.), Proceedings of the X International Symposium on Olfaction and Taste, Oslo.

Murlis, J., Elkinton, J.S., Cardé, R.T., 1992. Odor plumes and how insects use them. Annual Review of Entomology, 505–532.

Nabatiyan, A., Poulet, J.F.A., de Polavieja, G.G., Hedwig, B., 2003. Temporal pattern recognition based on instantaneous spike rate coding in a simple auditory system. Journal of Neurophysiology 90, 2484–2493.

Niehaus, M., 1981. Flight and flight control by the antennae in the small tortoiseshell (*Aglais urticae* L, Lepidoptera). II. Flight mill and free flight experiments. Journal of Comparative Physiology A 145, 257–264.

Olberg, R.M., 1983. Parallel encoding of direction of wind, head, abdomen, and visual pattern movement by single interneurons in the dragonfly. Journal of Comparative Physiology A 142, 27–41.

Olberg, R.M., Willis, M.A., 1990. Pheromone-modulated optomotor response in male gypsy moths, *Lymantria dispar* L.: directionally selective visual interneurons in the ventral nerve cord. Journal of Comparative Physiology A 167, 707–714.

Pichon, J.-M., Blanes, C., Franceschini, N., 1989. Visual guidance of a mobile robot equipped with a network of self-motion sensors. SPIE Mobile Robots IV 1195, 44–53.

Pollack, G.S., 1986. Discrimination of calling song models by the cricket, *Teleogryllus oceanicus*: the influence of sound direction on neural encoding of the stimulus temporal pattern and on phonotactic behaviour. Journal of Comparative Physiology A 158, 549–561.

Pollack, G.S., 2001. Analysis of temporal patterns of communication signals. Current Opinion in Neurobiology 11, 734–738.

Pollack, G.S., Hoy, R., 1981. Phonotaxis to individual components of a complex cricket calling song. Journal of Comparative Physiology A 144, 367–373.

Reeve, R., Webb, B., 2003. Neural circuits for robot phonotaxis. Philosophical Transactions of the Royal Society of London B 361, 2245–2266.

Restrepo, D., Teeter, J.H., Schild, D., 1995. Second messenger signalling in olfactory transduction. Journal of Neurobiology 30, 37–48.

Robert, D., Rowell, C.H.F., 1992. Locust flight steering. 2. Acoustic avoidance maneuvers and associated head movements, compared with correctional steering. Journal of Comparative Physiology a-Sensory Neural and Behavioral Physiology 171(1), 53–62.

Russell, R.A., 1999. Odour Detection by Mobile Robots, World Scientific Publishing Company, Singapore.

Russell, R.A., Thiel, D., Deveza, R., Mackay-Sim, A., 1995. A robotic

system to locate hazardous chemical leaks. IEEE International Conference on Robotics and Automation, 556–561.

Rust, M.K., Burk, T., Bell, W.J., 1976. Pheromone-stimulated locomotory and orientation responses in the American cockroach. Animal Behaviour 24, 52–67.

Rutkowski, A.J., Edwards, S., Willis, M.A., Quinn, R.D., Causey, G.C., 2004. A robotic platform for testing moth-inspired plume tracking strategies, International Congress of Robotics and Automation.

Sandini, G., Lucarini, G., Varoli, M., 1993. Gradient driven self-organizing systems. Proceedings of the IEEE/RSJ International Conference on Intelligent Robots and Systems, 429–432.

Saul, A.B., Humphrey, A.L., 1990. Spatial and temporal response properties of lagged and nonlagged cells in cat lateral geniculate nucleus. Journal of Neurophysiology 64, 206–224.

Schildberger, K., 1984. Temporal selectivity of identified auditory interneurons in the cricket brain. Journal of Comparative Physiology A 155, 171–185.

Schildberger, K., Hörner, M., 1988. The function of auditory neurons in cricket phonotaxis. 1. Influence of hyperpolarization of identified neurons on sound localization. Journal of Comparative Physiology A 163, 621–631.

Schmitz, B., Scharstein, H., Wendler, G., 1982. Phonotaxis in *Gryllus campestris* L. I Mechanism of acoustic orientation in intact female cricket. Journal of Comparative Physiology A 148, 431–444.

Schöne, H., 1984. Spatial Orientation, Princeton University Press, Princeton, NJ.

Schöning, M.J., Schütz, S., Schroth, P., Weissbecker, B., Steffen, A., KordoŤ, P., Hummel, H.E., Lüth, H., 1998. A bio-FET on the basis of intact insect antennae. Sensors and Actuators B 47, 235–238.

Schütz, S., Schöning, M.J., Schroth, P., Malkoc, Ü., Weissbecker, B., KordoŤ, P., Lüth, H., Hummel, H.E., 2000. An insect-based bioFET as a bioelectronic nose. Sensors and Actuators B 65, 291–295.

Shields, V., Hildebrand, J.G., 2001. Recent advances in insect olfaction, specifically regarding the morphology and sensory physiology of antennal sensilla of the female sphinx moth *Manduca sexta*. Microscopy Research and Technique 55, 307–329.

Sobel, E.C., Tank, D.W., 1994. In vivo Ca^2 dynamics in a cricket auditory neuron: an example of chemical computation. Science 263, 823–826.

Srinivasan, M.S., Bernard, G.D., 1977. The pursuit response of the housefly and its interaction with the optomotor response. Journal of Comparative Physiology 115, 101–117.

Stabel, J., Wendler, G., Scharstein, H., 1989. Cricket phonotaxis: localization depends on recognition of the calling song pattern. Journal of Comparative Physiology A 165, 165–177.

Staudacher, E.M., 2001. Sensory responses of descending brain neurons in the walking cricket, *Gryllus bimaculatus*. Journal of Comparative Physiology A 187, 1–17.

Staudacher, E.M., Schildberger, K., 1998. Gating of sensory responses of descending brain neurones during walking in crickets. Journal of Experimental Biology 201, 559–572.

Stout, J.F., McGhee, R., 1988. Attractiveness of the male *Acheta domestica* calling song to females II. The relative importance of syllable period, intensity and chirp rate. Journal of Comparative Physiology A 164, 277–287.

Strausfeld, N.J., 1976. Atlas of an Insect Brain, Springer, Berlin.

Strausfeld, N.J., Hansen, L., Li, Y.S., Gomez, R.S., Ito, K., 1998. Evolution, discovery, and interpretations of arthropod mushroom bodies. Learning and Memory 5, 11–37.

Sun, H., Frost, B.J., 1998. Computation of different optical variables of looming objects in pigeon nucleus rotundus neurons. Nature Neuroscience 1, 296–303.

Sutton, O.G., 1953. Micrometeorology, McGraw-Hill, New York.

Tammero, L.T., Dickinson, M.H., 2002. Collision-avoidance and landing responses are mediated by separate pathways in the fruit fly, *Drosophila melanogaster*. Journal of Experimental Biology 205, 2785–2798.

Thorson, J., Weber, T., Huber, F., 1982. Auditory behaviour of the cricket II. Simplicity of calling-song recognition in *Gryllus* and anomalous phonotaxis at abnormal carrier frequencies. Journal of Comparative Physiology A 146, 361–378.

Vickers, N.J., Baker, T.C., 1991. The effects of unilateral antennectomy on the flight behaviour of male *Heliothis virescens* in a pheromone plume. Physiological Entomology 16, 497–506.

Vickers, N.J., Baker, T.C., 1992. Male *Heliothis virescens* maintain upwind flight in response to experimentally pulsed filaments of their sex pheromone (Lepidoptera: Noctuidae). Journal of Insect Behavior 7, 669–687.

Vickers, N.J., Baker, T.C., 1994. Reiterative responses to single strands of odor promote sustained upwind flight and odor source location by moths. Proceedings of the National Academy of Sciences USA 91, 5756–5760.

Vickers, N.J., Baker, T.C., 1997. Flight of *Heliothis virescens* males in the field in response to sex pheromone. Physiological Entomology 22, 277–285.

Vickers, N.J., Christensen, T.A., Baker, T.C., Hildebrand, J.G., 2001. Odour-plume dynamics influence the brain's olfactory code. Nature 410, 466–470.

Voshall, L.B., Wong, A.M., Axel, R., 2000. An olfactory sensory map in the fly brain. Cell 102, 147–159.

Wagner, H., 1982. Flow-field variables trigger landing in flies. Nature 297, 147–148.

Wagner, H., 1986. Flight performance and visual control of flight of the free-flying housefly *Musca domestica* J. II. Pursuit of targets. Philosophical Transactions of the Royal Society of London B 312, 553–579.

Wandell, B.A., 1995. Foundations of Vision, Sinauer Associates, Sunderland, MA.

Warzecha, A.-K., Egelhaaf, M., 1996. Intrinsic properties of biological motion detectors prevent the optomotor control system from getting unstable. Philosophical Transactions of the Royal Society of London B 351, 1579–1591.

Webb, B., 2000. What does robotics offer animal behaviour? Animal Behaviour 60, 545–558.

Webb, B., 2002. Can robots make good models of biological behaviour? Behavioural and Brain Sciences 24, 1033–1050.

Webb, B., 2004. Neural mechanisms for prediction: do insects have forward models? Trends in Neurosciences 27, 278–282.

Webb, B., Harrison, R.R., 2000a. Eyes and ears: combining sensory motor systems modelled on insect physiology, IEEE International Conference on Robotics and Automation, San Francisco, April 24–28, pp. 3913–3918.

Webb, B., Harrison, R.R., 2000b. Integrating sensorimotor systems in a robot model of cricket behavior, Sensor Fusion and Decentralised Control in Robotic Systems III, November 6–8, SPIE, Boston.

Webb, B., Reeve, R., 2003. Reafferent or redundant: Integration of phonotaxis and optomotor behaviour in crickets and robots. Adaptive Behaviour 11, 137–158.

Webb, B., Scutt, T., 2000. A simple latency dependent spiking neuron model of cricket phonotaxis. Biological Cybernetics 82, 247–269.

Webb, B., Reeve, R., Horchler, A., Quinn, R., 2003. Testing a model of cricket phonotaxis on an outdoor robot platform, Towards Intelligent Mobile Robotics (TIMR '03) UWE Bristol, 28–29 August.

Weber, T., Thorson, J., 1988. Auditory behaviour in the cricket IV Interaction of direction of tracking with perceived temporal pattern in split-song paradigms. Journal of Comparative Physiology A 163, 13–22.

Weckström, M., Juusola, M., Laughlin, S.B., 1992. Presynaptic enhancement of signal transients in photoreceptor terminals in the compound eye. Proceeding of the Royal Society of London B 250, 83–89.

Weissburg, M.J., 2000. The fluid dynamical context of chemosensory behavior. Biological Bulletin 198, 188–200.

Wendler, G., 1990. Pattern recognition and localization in cricket phonotaxis, Sensory Systems and Communication in Arthropods, Birkhauser, Basel.

Willis, M.A., Arbas, E.A., 1991. Odor-modulated upwind flight in *Manduca sexta*. Journal of Comparative Physiology A. 169, 427–440.

Willis, M.A., Arbas, E.A., 1997. Active behavior and reflexive responses: another perspective on odor-modulated locomotion. In: Cardé, R.T., Minks, A.K. (Eds.), Pheromone Research: New Directions, Chapman and Hall, New York, pp. 304–319.

Willis, M.A., Baker, T.C., 1994. Behaviour of oriental fruit moth males during approach to sex pheromone sources. Physiological Entomology 19, 61–69.

Willis, M.A., Belanger, J., Jouse, W.C., 2002. Olfactory orientation in animals: hypothesis testing with a mobile robot. Society for Neuroscience. Abstracts 28, 4655.

Wohlers, D.W., Huber, F., 1981. Processing of sound signals by six types of neurons in the prothoracic ganglion of the cricket, *Gryllus campestris* L. Journal of Comparative Physiology 146, 161–173.